Network effects of eslicarbazepine in the hippocampus

Dissertation

zur

Erlangung des Doktorgrades (Dr. rer. nat.)

der

Mathematisch-Naturwissenschaftlichen Fakultät

der

Rheinischen Friedrich-Wilhelms-Universität Bonn

Vorgelegt von

Sarah Andrea Schmidt

Aus Köln

Bonn, 2019

Angefertigt mit Genehmigung der Mathematisch-Naturwissenschaftlichen Fakultät der Rheinischen Friedrich-Wilhelms-Universität Bonn

1. Gutachter: Prof. Dr. Heinz Beck
2. Gutachter: Prof. Dr. Walter Witke

Fachnahes Mitglied: Prof. Dr. Jörg Höhfeld

Fachfremdes Mitglied: Prof. Dr. Christa Müller

Tag der Promotion: 08.05.2020

Erscheinungsjahr: 2020

Abstract

Nearly 50 million people worldwide suffer from epilepsy, with 1/3 of the patients remaining without seizure control. This high number emphasizes the importance to develop new anti-epileptic drugs (AEDs) and to understand their mechanism. Many AEDs target voltage-gated sodium channels (VGSCs) in neurons of the brain, and the effects on a single cell basis is well studied. However, how AEDs act on the level of neuronal networks in the normal and epileptic brain is much less understood. Therefore, I investigated the effects of the new AED eslicarbazepine (S-Lic), the active metabolite of eslicarbazepine acetate on different types of excitatory and inhibitory neurons, as well as on feed-back and feed-forward inhibitory motifs in the CA1 area of the hippocampus. I performed my experiments in hippocampal slices from both sham-control and pilocarpine-treated chronically epileptic rats. I found that 300 µM S-Lic significantly reduces maximal firing rates in CA1 pyramidal cells, as well as in putative feed-forward interneurons located in the CA1 stratum radiatum and in putative feed-back interneurons located in stratum oriens of CA1. Consequently, S-Lic reduced feed-forward inhibition in both sham-control and epileptic animals. However, S-Lic did not reduce feed-back inhibition but resulted in a plastic upregulation of feed-back inhibitory postsynaptic currents (IPSCs) only in epileptic and not in sham-control animals. I showed that this plastic upregulation is dependent on Ca^{2+} permeable AMPA receptors (CP-AMPAR) and relies on an anti-Hebbian LTP mechanism. Indeed, this type of LTP has been described previously for inhibitory feed-back interneurons. In summary, my results show that S-Lic, in contrast to other AEDs, affects inhibitory circuits in the CA1 hippocampal region also in epileptic tissue. Therefore, AEDs mechanism of action may not be fully explained by direct actions on their target channels and on a single cell level. Additionally, it is necessary to investigate long-term effects of AEDs on microcircuits in the brain.

Zusammenfassung

1 % aller Menschen erkranken im Laufe ihres Lebens an einer Epilepsie. Dabei treten wiederholt Anfälle auf, die durch gezielte Behandlung therapiert werden können. Unterschiedliche Epilepsien können unterschiedlich gut behandelt werden, so werden bei manchen Formen der Epilepsie bis zu 90 % der Betroffenen anfallsfrei, bei anderen jedoch nur 30 %. Patienten, deren Anfälle nicht mit verfügbaren Antiepileptika verhindert werden können scheinen pharmakoresistent zu sein. Um Betroffene besser therapieren zu können, ist es deswegen wichtig die Wirkungsmechanismen von Antiepileptika weiter zu untersuchen. Viele Antiepileptika wirken auf spannungsabhängige Natrium Kanäle und der Wirkmechanismus auf diese wurde umfangreich untersucht. Allerdings wurde bisher wenig die Wirkung von Antiepileptika auf neuronale Netzwerke im gesunden und erkrankten Gehirn erforscht. Daher habe ich mich in meiner Doktorarbeit mit der Wirkung des Antiepileptikums Eslicarbazepine (S-Lic), dem aktiven Metaboliten von Eslicarbazepinesäure beschäftigt. Ich habe den Effekt von S-Lic auf verschiedene Typen von erregenden und hemmenden Neuronen und auf feed-back und feed-forward inhibierende Netzwerke untersucht. Für meine Experimente nutze ich hippocampale Gehirnschnitte von gesunden und mit Pilocarpin behandelte, chronisch epileptische Ratten. Mit Hilfe der patch-clamp Methode konnte ich zeigen, dass 300 µM S-Lic die maximale Feuerrate von CA1 Pyramidenzellen, sowie von putativen feed-forward und feed-back Interneuronen reduziert. Außerdem konnte ich zeigen, dass 300 µM S-Lic feed-forward Inhibition in Kontroll- und epileptischen Tieren reduziert. Im Gegensatz dazu reduziert S-Lic nicht die feed-back Inhibition, sondern potenziert feed-back inhibitorische post-synaptische Ströme nur in epileptischen Tieren und nicht in Kontrolltieren. Ich habe gezeigt, dass diese Potenzierung abhängig von CP-AMPAR ist und auf Mechanismen der anti-Hebbschen Langzeitpotenzierung (LTP) beruht. Interessanterweise wurde diese anti-Hebbsche LTP schon in inhibitorischen feed-back Interneuronen entdeckt.

Zusammenfassend konnte ich zeigen, dass S-Lic im Gegensatz zu anderen Antiepileptika eine Wirkung auf inhibierende Netzwerke in epileptischen Gewebe in der CA1 Region des Hippocampus hat. Diese Arbeit zeigt, dass

Wirkungsmechanismen von Antiepileptika nicht ausschließlich durch deren direkte Wirkung auf primäre Zielstrukturen, wie Ionenkanäle, und auf Einzelzellebene zu erklären sind. Zusätzlich ist es nötig Langzeiteffekte von Antiepileptika auf Mikronetzwerke im Gehirn zu untersuchen.

Contents

1. Introduction

1.1. Epilepsy

Epilepsy is a chronic neurologic disorder that affects nearly 50 million people worldwide (WHO, 2018). It is a disorder of the brain characterized by an enduring predisposition to generate epileptic seizures. The definition of epilepsy requires at least one unprovoked seizure (Fisher et al., 2005, 2014). An epileptic seizure is the transient occurrence of symptoms, like disturbed sensory, motor or autonomic function, due to abnormal, hyperactive or synchronous neuronal activity (Fisher et al., 2005). In 2017 the International League Against Epilepsy (ILAE) presented a new classification of the epilepsies. This classification presents three levels, first the seizure type, second the diagnosis of epilepsy type and finally the epilepsy syndrome. The first level of the classification describes seizure types, which can be classified by the initial manifestation of the seizure either being focal, generalized or unknown. Focal seizures originate within networks of one hemisphere and can spread within local networks of one hemisphere as well as extend bilaterally. Furthermore, focal seizures can show motor symptoms like automatisms or hyperkinetic movements and nonmotor symptoms like cognitive seizures including impaired language, hallucinations or perceptual distortions (Fisher et al., 2018b; Scheffer et al., 2018). For focal seizures, the patients level of awareness can be included in the classification of the seizure type. Generalized seizures can be divided into motor and nonmotor seizures (Fisher et al., 2018b; Scheffer et al., 2018). Motor seizures include e.g. tonic or tonic clonic seizures with symptoms ranging from extension or flexion postures to rhythmically jerking (Fisher et al., 2018a). Nonmotor seizures classified within generalized seizures are also termed absences. An absence seizure can be characterized e.g. by hyperventilation, arrest of activity, staring and loss of responsiveness (Scheffer et al., 2018). The second level of the ILAE classification describes different epilepsy types, including focal, generalized or combined generalized and focal epilepsies. Many of these include multiple types of seizures. E.g. focal epilepsies can include seizure types

like focal motor seizures, focal impaired awareness seizures or focal to bilateral tonic-clonic seizures (Scheffer et al., 2017). The third level characterizes epilepsy syndromes, which includes features as seizure types, electroencephalography (EEG) recordings as well as neuroimaging like magnetic resonance imaging (MRI). Epilepsy syndromes include well-recognized syndromes, like childhood absence epilepsy or the Dravet syndrome and others. Additional to these three levels, the new classification incorporates etiology of the patient's epilepsy, including structural, genetic, infectious, metabolic, immune and unknown etiologies. E.g. genetic etiology can be key for genetic counseling and consideration of novel drug therapies as well as structural etiology, which is critical for epilepsy surgery (Scheffer et al., 2017). In this study I will focus on one of the focal epilepsy types, mesial temporal lobe epilepsy.

1.1.1. Temporal lobe epilepsy

Mesial temporal lobe epilepsy (mTLE) is the most common form of epilepsy with focal seizures (Engel, 2001). At least 60-65 % of patients suffering from temporal lobe epilepsy show hippocampal sclerosis (HS) (Wiestler and Blümcke, 2002; Blümcke et al., 2013). The hippocampus is located in the medial temporal lobe and consists of the ammon's horn (Cornu Ammonis (CA)) and the dentate gyrus (DG) (Per et al., 2009, see **Figure 1A**). HS is characterized by cell loss of excitatory and inhibitory neurons, gliosis, i.e. proliferation or hypertrophy of glial cells, mossy fiber sprouting and dentate granule cell dispersion (Engel, 1996; Blümcke et al., 2013). The most common form of HS (HS type 1) affects 60-80 % of all TLE-HS cases reported (Taylor, 1989; Davies et al., 1996; MD et al., 2006; Blümcke et al., 2007). HS type 1 incorporates e.g. loss of excitatory cells such as > 80 % of pyramidal cells (PCs) within CA1, 30-50 % in CA2, 30–90 % of neurons in CA3, and 40–90 % of neurons in CA4 (Blümcke et al., 2012) and 50-60 % of granule cells in the dentate gyrus (Bratz, 1899; Margerison and Corsellis, 1966, see **Figure 1B**).

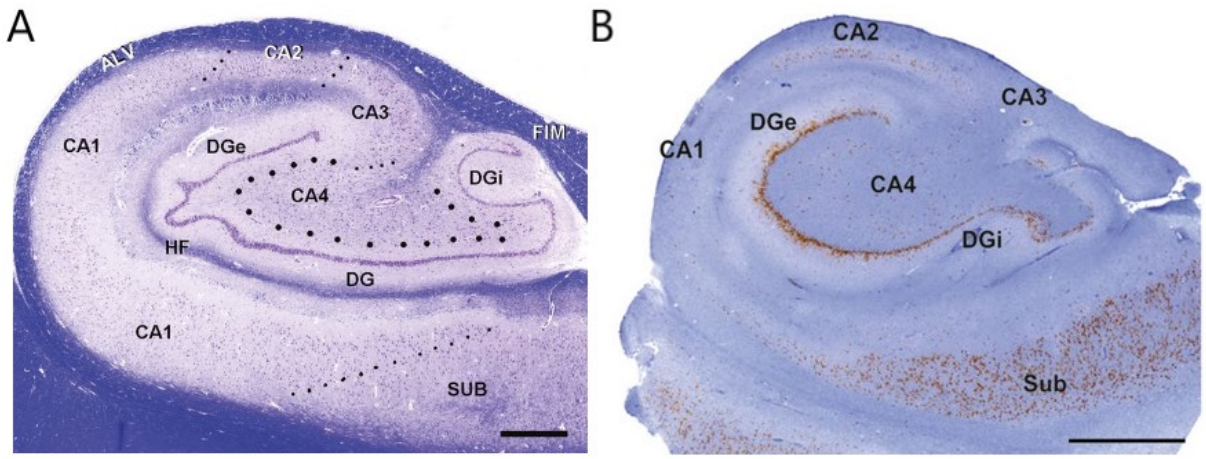

Figure 1: Microscopic anatomy of the human hippocampus and the histopathologic subtype of hippocampal sclerosis in patients with TLE. ***A*** Cresyl-violet and Luxol-Fast-Blue staining of a postmortem human hippocampus: SUB, subiculum; CA1–CA4, sectors of the Cornu ammonis; DG, dentate gyrus with external (DGe) and internal limbs (DGi); HF, remnant of hippocampal fissure; ALV, alveus; FIM, fimbria. Dotted lines circumscribe anatomic boundaries between CA sectors. ***B*** ILAE hippocampal sclerosis type 1 with pronounced pyramidal cell loss in both CA4 and CA1 sectors. Damage to sectors CA3 and CA2 is more variable, but frequently visible. Variable cell loss in the dentate gyrus, with abundant granule cell loss in the internal limb (DGi). Scale bars 1 µM. (Adapted from Blümcke et al. 2013)

As mentioned above, not only excitatory but also inhibitory cells can be lost after an epileptogenic insult. Several studies have shown that somatostatin-containing (SST positive OLM cells) interneurons seem to be the most vulnerable cell subpopulation to die after an epileptogenic insult (de Lanerolle et al., 1989; Buckmaster and Jongen-Rêlo, 1999; Cossart et al., 2001; Wittner et al., 2001; Dinocourt et al., 2003; Kobayashi and Buckmaster, 2003). Especially in the hilus and stratum oriens of CA1 the cell loss of OLM cells accounts for 83 % and for ~ 50 % of the total GABAergic cell loss (Buckmaster and Jongen-Rêlo, 1999; Dinocourt et al., 2003, see **Figure 2A, B**). Additionally, parvalbumin-containing interneurons, which target perisomatically PCs, degenerate in the hippocampus (DeFelipe, 1999; Cossart et al., 2001; Sayin et al., 2003; Van Vliet et al., 2004, see **Figure 2C, D**).

To study TLE pathophysiology and to develop new therapeutic approaches, different animal models of temporal lobe epilepsy have been developed. One of these models uses the chemoconvulsant muscarinic receptor agonist pilocarpine to induce an initial brain injury, which results in this case in a long and persistent seizure, the status epilepticus (SE). Initiation of the seizure is induced by the activation of the cholinergic system but the histopathology and spontaneous seizure activity is due to seizure-

induced glutamate release (Jope et al., 1986; Sloviter, 1987). Pilocarpine-induced SE leads e.g. to cell loss in the hilus of the dentate gyrus as well as in the hippocampal subfields CA1 and CA3 (Mello et al., 1993). Between 4-9 days after SE, supragranular sprouting of excitatory mossy fibers can be observed. This leads to de novo recurrent excitation of granule cells in the dentate gyrus and consequently to spontaneous recurrent seizures (Cavalheiro et al., 1991; Mello et al., 1993). Therefore, this model resembles some of the main features of human mTLE (Cavalheiro E.A., 1995).

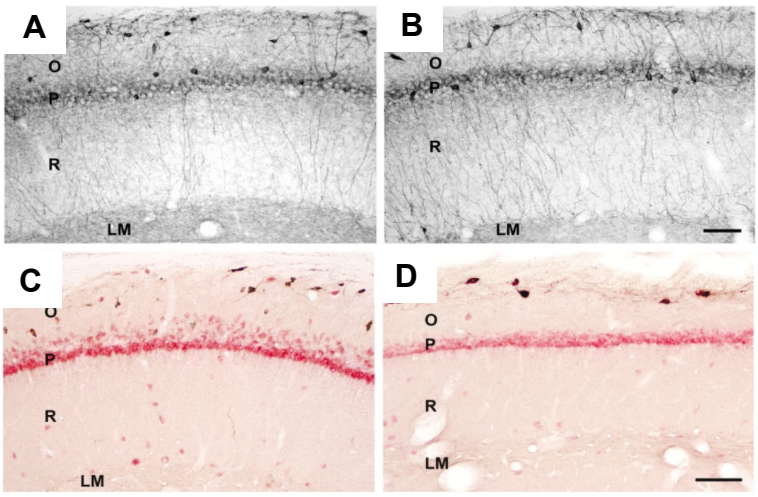

Figure 2: Loss of interneurons in epileptic tissue. ***A, B*** Immunohistochemical labeling for parvalbumin in the CA1 region for parvalbumin in control and pilocarpine treated rat respectively ***C, D*** Immunohistochemical labeling for somatostatin in the CA1 region for parvalbumin in control and pilocarpine treated rat respectively. (O) stratum oriens, (P) stratum pyramidale, (R) stratum radiatum, (LM) stratum lacunosum moleculare. Scale bar 100 µm. Adapted from Dinocourt et al., 2003)

1.2. Antiepileptic drugs

AEDs are able to prevent epileptic seizures and target different points of application in the brain. AEDs can act on voltage-gated calcium channels (Gee et al., 1996; Marais et al., 2001), the GABA system (Gallagher et al., 1978; Bormann et al., 1987; Akaike et al., 1989), or glutamate receptors (Subramaniam et al., 1995; Sheth and Gidal, 1998; Rogawski et al., 2003). One commonly used AED class are VGSC blockers like oxcarbazepine (OXZ), carbamazepine (CBZ) and eslicarbazepine (ESL) (Rogawski and Löscher, 2004). They mainly block VGSCs in a use-dependent manner (Macdonald and Kelly, 1995; Ragsdale and Avoli, 1998). These use-dependent blocking effects are important because they preferentially block prolonged high-frequency activity, which occurs during a seizure (Bragin et al., 1999).

1.2.1. Eslicarbazepine (S-Lic)

One novel VGSC blocker is eslicarbazepine acetate. This drug is structurally related to CBZ. Eslicarbazepine acetate is a once daily AED used to treat adults with focal-onset seizures. After oral administration it undergoes hydrolysis to its active metabolite eslicarbazepine (S-Lic, Almeida and Soares-da-Silva, 2007; Almeida et al., 2008; Maia et al., 2008; Gerlach and Krajewski, 2010, see **Figure 3**). AEDs like ESL and CBZ as well as local anesthetics bind to a common receptor site in the pore of the sodium channel. In general, VGSCs consist of four potential auxiliary subunits, β1 to β4, which modulate the kinetics and voltage dependence of channel gating as well as their pharmacology and the main α subunit, which is located in the transmembrane (Catterall, 2000; Uebachs et al., 2010; Brackenbury and Isom, 2011). AEDs and local anesthetics bind to the S6 segment in domains I, III and IV, that create a three-dimensional drug receptor site in the α subunit (Qu et al., 1995; Ragsdale et al., 1996; Catterall, 2014). S-Lic preferentially blocks VGSCs in rapidly firing neurons (Bonifácio et al., 2001).

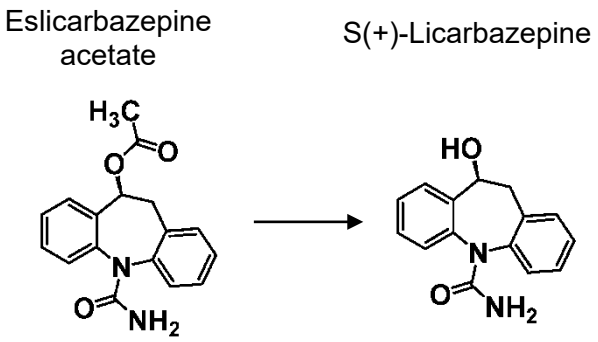

Figure 3: Structure of Eslicarbazepine. Eslicarbazepine acetate is converted to S-Licarbazepine. (adapted from Gerlach et al. 2010).

1.2.2. S-Lic effects on slow inactivation of VGSCs

An important feature of S-Lic is its greater selectivity for the inactive state of VGSC compared to other AEDs like CBZ (Hebeisen et al., 2011). The inactive state of VGSCs is induced by rapid firing in neurons. VGSCs activation is voltage dependent, consequently at resting membrane potential most sodium channels are in a resting and closed state. Upon depolarization, VGSCs open and conduct ions. After activation, channels convert into the inactivated state (Catterall, 2000). Recovery from inactivation is dependent on membrane repolarization. Fast inactivation and recovery within milliseconds is enabling neurons to fire rapid trains of action potentials. In contrast to

that, slow inactivation is in order of seconds and contributes to termination of burst firing (Goldin, 2003; Ulbricht, 2005; Oliva et al., 2012).

S-Lic is able to shift the voltage dependence of slow inactivation to more negative potentials and thereby reduces overall membrane excitability by increasing action potential thresholds (Soares-da-Silva et al., 2015; Holtkamp et al., 2018). S-Lic shows greater selectivity for the inactive state of VGSC (see above) but also alters slow inactivation of specific VGSC subtypes. In mammals, there are four different isoforms expressed in the adult brain, $Na_v1.1$-1.3 and $Na_v1.6$ (Trimmer and Rhodes, 2004; Vacher et al., 2008). The isoforms $Na_v1.2$ and $Na_v1.6$ are mainly expressed in excitatory cells of the brain, whereas $Na_v1.1$ is mainly expressed in GABAergic interneurons (Yu et al., 2006; Ogiwara et al., 2007). A recent study using expression systems showed that S-Lic affects slow inactivation only of $Na_v1.2$ and $Na_v1.6$, but not of $Na_v1.1$ and $Na_v1.3$ (Holtkamp et al., 2018). These results show that S-Lic blocks specific VGSCs subtypes.

1.2.3. Pharmacoresistance

Published data suggest that some AEDs like CBZ and phenytoin (PHT) show a loss of use-dependent blocking effects in chronic experimental epilepsy (Remy et al., 2003a, 2003b). This loss of use-dependent blocking can result in pharmacoresistance of the epileptic tissue. In human mTLE nearly 30 % of patients suffering from epilepsy are considered to be pharmacoresistant (Regesta and Tanganelli, 1999). However, the mechanism of pharmacoresistance has not been fully explained yet. Extensive research has been trying to resolve changes that occur after seizures, which could be responsible for the loss of drug response. Two main concepts have been discussed to explain the development of pharmacoresistance. The target hypothesis of pharmacoresistance suggests that a modification of the drug target can lead to a reduced efficacy of a given AED (Remy and Beck, 2006). VGSCs are targets for multiple first-line AEDs (Remy and Beck, 2006) and numerous changes in sodium channel subunit expression have been shown in experimental and human epilepsy (Bartolomei et al., 1997; Aronica et al., 2001; Whitaker et al., 2001; Ellerkmann et al., 2003). The second concept emphasizes the importance of AED concentration distribution in different compartments within the central nervous system (CNS). The transporter hypothesis states that an enhanced function of multidrug transporters, which control intraparenchymal AED concentration could lead to insufficient AED

levels in the intraparenchym and therefore lead to reduced drug effects (Kwan and Brodie, 2005, see **Figure 4**).

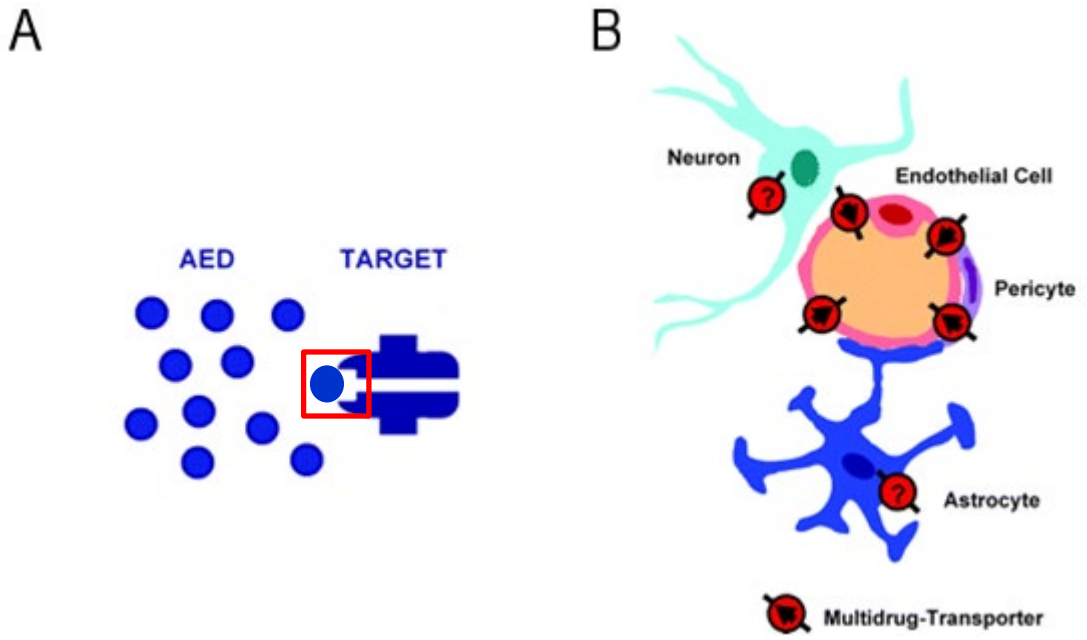

Figure 4: Two concepts of development of pharmacoresistance. ***A*** Target modifications could occur due to seizure-induced changes in transcription or alternative splicing of ion channel subunits, altered post-translational modification of the protein and/or phosphorylation by protein kinases. Modification of the drug target can result in reduced binding-efficacy of an AED ***B*** Increased expression or function of multidrug transporter proteins decreases availability of the AED at its target (Adapted from Remy and Beck, 2006)

1.2.4. AED effects on sodium channels in epileptic tissue

Moreover, when comparing S-Lic and CBZ in their effects in human derived tissue, it has been shown repeatedly that CBZ loses its use-dependent block of sodium channels (Remy et al., 2003a). A recent study by Beckonert et al. in 2018 gives a potential explanation for the use-dependent loss of CBZ in epileptic tissue. It has been shown that in epileptic tissue due to a change in polyamine metabolism, a decrease in spermine levels arises in epileptic hippocampus (Royeck et al., 2015). Beckonert et al. hypothesize that spermine binds in a cooperative manner with CBZ. They show that intracellular spermine restores efficacy of CBZ in epileptic tissue (Beckonert et al., 2018). In contrast to that, S-Lic still shows potent activity on sodium current recovery inactivation and discharge behavior in experimental epilepsy (Doeser et al., 2015). However, it remains elusive how S-Lic in contrast to CBZ still shows a use-dependent block of VGSCs in epileptic tissue.

1.2.5. S-Lic effects on persistent sodium currents

Transient sodium currents (I_{NaT}) carried out by VGSC are involved in the fast upstroke of action potentials and their termination. However, a small fraction of VGSC remain open, which is termed persistent sodium current (I_{NaP}). This persistent sodium current is an important modulator of membrane excitability and activates in the subthreshold voltage range (Magistretti and Alonso, 1999). The molecular basis for I_{NaP} depends on the subunit composition of the sodium channel. β subunits regulate trafficking and gating of sodium channels, especially β2 and β3 modulate persistent sodium current (Isom et al., 1995; Qu et al., 2001). β subunit mutations have been shown to affect kinetics and voltage dependence of channel gating with the result of hyperpolarized membrane potentials and reduced sodium channel rundown during high-frequency channel activity (Meadows et al., 2002). Interestingly, I_{NaP} has been shown to be increased in animal models of chronic epilepsy (Chen et al., 2010). This modulation of I_{NaP} in chronic epilepsy is associated with sodium channel mutations (Stafstrom, 2007). Still, the role of β subunits in chronic epilepsy is not yet understood, but is one potential candidate to investigate effects of AEDs on e.g. persistent sodium current. A study investigating the effects of CBZ on persistent sodium currents in a mouse model lacking the β1 subunit of sodium channels showed that CBZ still reduces transient sodium currents but paradoxically increased persistent sodium currents. This effect leads to a complete loss of efficacy in reducing repetitive firing (Uebachs et al., 2010). The effects of S-Lic on persistent sodium currents were tested in a mouse line lacking either the β1 or the β2 subunit. In contrast to CBZ, S-Lic did not cause a paradoxical upregulation of I_{NaP}, but was able to reduce maximal I_{NaP} conductance and thereby efficiently decreased firing rate (Doeser et al., 2014). These studies suggest that S-Lic seems to have a different mechanism of action than CBZ. Especially, S-Lic in contrast to CBZ seems to overcome cellular resistance mechanisms in epileptic tissue, by effectively reducing maximal I_{NaP} conductance as well as reducing neuronal firing even in mice lacking specific β subunits (Doeser et al., 2014).

1.3. Hippocampal inhibitory microcircuits

As mentioned in 1.1.1, the hippocampus is next to other structures the origin of seizures in mTLE (Engel, 2001). To study the effects of AEDs on the hippocampus it is important to understand its network connectivity. In mTLE, it has been shown that, CA1 area of the hippocampus can be directly recruited from entorhinal cortex into the epileptic network and participate in seizure spread (Barbarosie et al., 2000; Sari and

Kerr, 2001; Wozny et al., 2005; Ang et al., 2006). To restrict seizure spread, functional inhibitory microcircuits within CA1 play an important role (Benini and Avoli, 2005; Orman et al., 2008). These inhibitory microcircuits and inhibitory inputs on principal cells are mediated by inhibitory interneurons. Most of these interneurons act via the main inhibitory neurotransmitter γ-aminobutyric acid (GABA) and lead to hyperpolarization of the postsynaptic cell due to influx of chloride. Inhibitory interneurons represent a very diverse neuronal population with at least 21 different subtypes in the hippocampus (Freund and Buzsáki, 1996). Interneurons differ in their set of process morphology, physiological properties and expression profile of different molecules and receptors (Freund and Buzsáki, 1996; McBain and Fisahn, 2001; Maccaferri and Lacaille, 2003; Ascoli et al., 2008). The axon morphology can be used to classify interneuron subtypes. In general, a differentiation is made between interneurons targeting perisomatic or dendritic compartments (Han et al., 1993; Buhl et al., 1994). Perisomatic interneurons include axo-axonic cells, which innervate the axon initial segments and basket cells, which target the soma of principal cells (Somogyi et al., 1983; Buhl et al., 1994; Freund and Buzsáki, 1996; Halasy et al., 1996). Perisomatic interneurons are able to control action potential output of their target cells, control spike timing and are involved in synchronization during oscillatory events (Chrobak and Buzsáki, 1995; Pouille and Scanziani, 2001a; Freund and Katona, 2007; Losonczy et al., 2010). Dendritic targeting interneurons can be classified by different dendritic compartments they innervate. Bistratified cells and Schaffer collateral-associated cells target proximal dendrites in stratum oriens and radiatum (Buhl et al., 1994; Cossart et al., 1998). Oriens-lacunosum moleculare (OLM) interneurons have their soma in stratum oriens and target the distal apical tuft of PCs in stratum lacunosum moleculare (Sik et al., 1995). Additionally, perforant path-associated and neurogliaform cells, which have their soma in stratum radiatum and stratum lacunosum moleculare target the distal apical tuft (Hájos and Mody, 1997; Cossart et al., 1998; Vida et al., 1998). Consequently, dendritic targeting interneurons are involved in shaping and controlling excitatory inputs, which impinge on the same dendritic compartments (McBain and Fisahn, 2001). Finally, there are also other interneuron types like trilaminar cells, which innervate more than one dendritic compartment (Sik et al., 1995; Klausberger et al., 2005).

The spatial and temporal inhibition of principal cells mediated by inhibitory interneurons depends also on the activation profile of these interneurons. Depending on the inputs interneurons receive, they can be assigned to different networks motifs. One of these inhibitory motifs is called feed-back inhibition. Feed-back inhibition requires excitatory neurons to drive inhibitory interneurons, which in turn inhibit the same population of excitatory neurons. Activation of e.g. CA1 PCs can lead to an activation of inhibitory interneurons which innervate the principal cells in a feed-back loop. Interneurons involved in this network are basket cells like parvalbumin-positive (fast-spiking PV+) and cholecystokinin-positive (regular spiking CCK+), which innervate perisomatically CA1 PCs (Kullmann, 2011) but mainly OLM cells, which are mostly somatostatin positive (SST positive OLM cells). OLM cells receive their main input in stratum oriens from CA1 PCs and target these at their distal dendrites in stratum lacunosum moleculare (see **Figure 5A**, Blasco-Ibáñez and Freund, 1995). Interneurons involved in feed-back inhibition are not only activated by the CA1 PC itself, but also receive excitatory inputs from Schaffer collaterals of CA3 axons. Basket cells receive this input and can therefore also participate in feed-forward inhibition. In feed-forward inhibition, excitatory neurons drive inhibitory cells, which in a downstream pathway inhibit a population of postsynaptic excitatory neurons. E.g., interneurons with their soma in stratum radiatum of CA1 (Schaffer-collateral-associated interneurons) receive Schaffer collateral inputs from CA3 and inhibit CA1 PCs at their proximal dendrites (Klausberger, 2009, see **Figure 5B**).

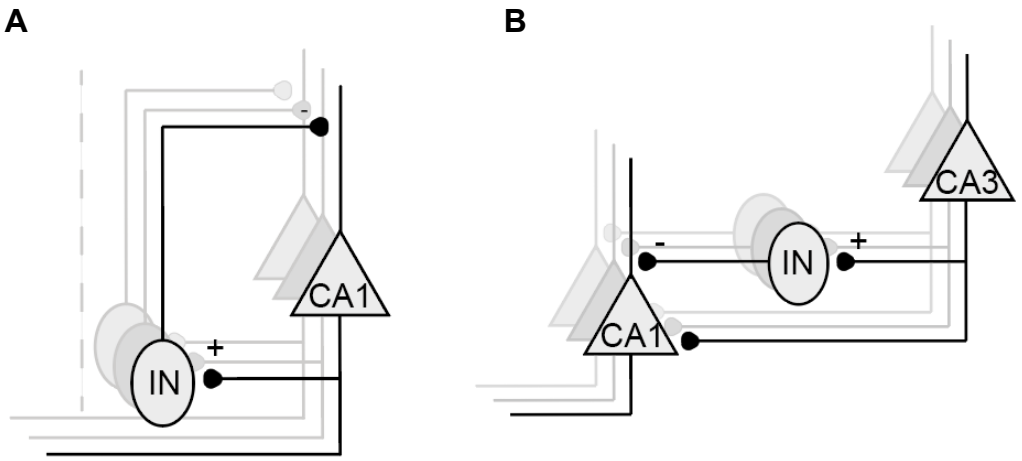

Figure 5: Feed-back and feed-forward inhibition in hippocampal microcircuits. ***A*** An activation of e.g. CA1 PCs can lead to activation of inhibitory interneurons, which back project onto the CA1 PC via a GABAergic synapse. ***B*** Activation of e.g. axons of CA3 PCs (Schaffer collaterals) which activate inhibitory interneurons, which themselves project via a GABAergic synapse onto CA1 PCs.

1.3.1. Plasticity at synapses of interneurons

Because the hippocampus and its networks are highly associated with learning, plasticity of cells and networks is necessary. How are these heterogeneous interneuron types involved in different types of plasticity? Two types of long term plasticity (LTP) have been described for interneurons in the hippocampus. In nearly all interneuron types a *N*-Methyl-$_D$-aspartate (NMDA) -receptor dependent LTP (Hebbian LTP) has been found (Hebb, 1949; for reviews see Bi and Poo, 2001 and Kullmann and Lamsa, 2007). For this type of LTP a pairing of presynaptic tetanic stimulation with postsynaptic depolarization is necessary to remove the magnesium block of NMDA-receptors (Hebb, 1949). The second type of LTP is dependent on Ca^{2+}-permeable α-amino-3-hydroxy-5-methyl-4-isoxazolepropionic acid (AMPA) receptors (CP-AMPAR) and is called Anti-Hebbian LTP. This type of plasticity is only possible due to a lack of a specific AMPAR subunit. AMPAR are expressed in principal cells and in most interneuron types and contain to a high extent the glutamate receptor 2 (GluR2) subunit. GluR2 subunits contain at a critical position (Q/R site) in the putative membrane segment 2 a positively charged arginine (R) residue instead of a neutral glutamine (Q) residue at this site in GluR1, GluR3 and GluR4 subunits. The positively charged arginine residue in GluR2 subunits makes the channel impermeable to Ca^{2+}. Channels which lack to a high extent the AMPAR GluR2 subunit are permeable to Ca^{2+} and are susceptible to voltage-dependent block by polyamines (Donevan and Rogawski, 1995). Because polyamines are positively charged, they block the pore of the channel during depolarization (Bowie and Mayer, 1995; Koh et al., 1995). Therefore, CP-AMPAR dependent LTP is only possible if the postsynapse is hyperpolarized. Interestingly Anti-Hebbian LTP has been shown to occur in the hippocampus only in OLM cells, which participate mainly in feed-back inhibition (Lamsa et al., 2007a). In respect of AED effects on different types of neurons, it would be interesting to investigate whether S-Lic affects synaptic plasticity at all or if it affects synaptic plasticity differently depending on the type of synaptic plasticity.

1.4. Aims and objectives

Mesial temporal lobe epilepsy is a severe neurological disorder with 30 % of patients remaining pharmacoresistant. This high number emphasizes the need to develop new AEDs and to understand their mechanism of action. So far not many studies have investigated the effects of AEDs on a network level. A recent study investigated the effects of CBZ on inhibitory hippocampal networks (Pothmann et al., 2014). They found

that the two inhibitory motifs of feed-back and feed-forward inhibition in hippocampal CA1 area were unaffected by CBZ and additional commonly used Na^+ channel-acting anticonvulsants in control and epileptic animals (Pothmann et al., 2014). However their data shows that intrinsic firing of different inhibitory interneurons (basket cells, bistratified cells innervating the proximal dendrites of PCs (PD) and OLMs) is reduced during presence of CBZ, but synaptic recruitment of these interneurons during network activity is not sufficient for the development of a use-dependent Na^+ channel block by CBZ (Pothmann et al., 2014). As mentioned in 1.2.1, S-Lic seems to have a different mechanism of action in comparison to CBZ. It would be interesting to investigate the effects of S-Lic not only on single cell level, but also on inhibitory networks in the hippocampus.

Therefore, I investigated the effects of the AED eslicarbazepine acetate on inhibitory micronetworks in the hippocampus in control and epileptic tissue. Using the pilocarpine model of epilepsy, I investigated the effects of S-Lic on feed-forward and feed-back inhibition in the CA1 area of the hippocampus. With the patch-clamp technique I was able to investigate the effects of S-Lic on feed-forward inhibition, with stimulation of CA3 Schaffer collaterals and recordings of IPSCs in CA1 PCs, as well as excitatory postsynaptic currents (EPSCs) in feed-forward interneurons with their soma in stratum radiatum. Additionally, I recorded action potential firing of CA3 PCs during CA3 axon stimulation. To investigate feed-back inhibition in CA1, I stimulated within the alveus of CA1 area and recorded IPSCs in CA1 principal cells as well as excitatory postsynaptic potentials (EPSPs) in feed-back interneurons with their soma in stratum oriens. To investigate the effects of S-Lic on intrinsic properties of CA1 principal cells and feed-forward as well as feed-back interneurons, I recorded current injection induced action potential firing.

2. Material & Methods

2.1. Pilocarpine model of epilepsy

The pilocarpine model of epilepsy was used for all slice experiments with chronic epileptic animals. Male Wistar rats (150–180 g) were injected intraperitoneally with pilocarpine hydrochloride (340 mg/kg body weight; Sigma-Aldrich) 30 min after a subcutaneous injection of 1 mg/kg scopolamine methyl nitrate (Sigma-Aldrich) to reduce peripheral cholinergic side effects of pilocarpine. About 50 % of pilocarpine-injected animals developed a limbic SE that was terminated by injection of 1 ml of diazepam 40 min after onset (0.5 %; Ratiopharm). In animals that did not develop SE after the first injection, a second identical dose of pilocarpine was administered. 40 min after SE, rats received an injection of 1 ml 0.5 % diazepam (Ratiopharm), and finally two subcutaneous injections of each 1 ml Ringer's and 5 % glucose solution. Animals were housed individually in separate cages with 12 hrs/7 d video monitoring for 4 weeks after SE. Only rats displaying at least one spontaneous seizure during this period were included in this study. Experiments were conducted 4–8 weeks after SE. Sham-control animals were treated in an identical manner, only the pilocarpine injection was omitted. In this study, sham-control and untreated age-matched Wistar rats (40 % and 60 %, respectively) were pooled. All animal experiments were conducted in accordance with the guidelines of the Animal Care and Use Committees of the University of Bonn und the county of North-Rhine Westphalia (AZ 84-02.04.2015.A524).

2.2. Brain slice preparation and patch-clamp recording

Transverse 300 µM thick hippocampal slices were prepared on a vibratome (Leica VT 1200S) in ice-cold preparation solution containing (in mM) 60 NaCl, 100 sucrose, 2.5 KCl, 1.25 NaH_2PO_4, 26 $NaHCO_3$, 1 $CaCl_2$, 5 $MgCl_2$, and 20 D-glucose (equilibrated with 95 % O_2 and 5 % CO_2). Slices were first stored in the preparation solution for 30 min at 35°C and then transferred to artificial cerebrospinal fluid (ACSF) containing (in mM) 125 NaCl, 3 KCl, 1.25 NaH_2PO_4, 26 $NaHCO_3$, 2.6 $CaCl_2$, 1.3 $MgCl_2$, and 15 D-

glucose (equilibrated with 95 % O_2 and 5 % CO_2) for storage at room temperature. For recordings, single slices were transferred to a submerged chamber perfused with ACSF (1.5 ml per minute) and mounted on the stage of an upright microscope (Axioscope 2; Zeiss). Cells were visualized by infrared oblique illumination optics through a water-immersion objective (60X, 0.9 NA; Olympus) with a CCD camera (Hamamatsu). Somatic whole-cell recordings of principal cells and interneurons in the CA1 region were obtained with a BVC-700A (Dagan) or Multiclamp 700B amplifier (Molecular devices). Data were lowpass filtered (10 kHz) and sampled at 100 kHz with a Digidata 1440A or 1550 interface controlled by pClamp software (Molecular Devices). Recording electrodes were made from thick-walled borosilicate glass capillaries (GB 150F 8P; Science Products) on a vertical puller (PP-830; Narishige). Recording pipettes for whole-cell recordings had a resistance of 3–6 MΩ when filled with (in mM) 140 K-Gluconate, 5 4-(2-hydroxyethyl)-1-piperazineethanesulfonic acid (HEPES), 0,16 ethylene glycol-bis (β-aminoethyl ether)-N,N,N′,N′-tetraacetic acid (EGTA), 0,5 $MgCl_2$, 5 Phosphocreatine Na_2 (pH 7.35, adjusted with sucrose to 292 mOsm). For recordings from interneurons, 0,3 % Biocytin was added to this solution to achieve post-recording morphologic reconstruction. Pipettes for loose-patch recording had a resistance of 7 – 10 MΩ and were filled with ACSF. All experiments were performed at 33°C. Membrane potential was corrected offline for a liquid junction potential of -15.95 mV.

2.3. Biocytin reconstructions

Slices containing biocytin-filled cells were incubated at room-temperature in formaldehyde (4 % in 0.1 phosphate buffered saline (PBS), pH 7.4) for one hour. After wash with PBS, slices were permeabilized overnight at 4 °C with Triton X-100 (0.4 % in PBS) and on the next day incubated for 2 h at room-temperature in Strepavidin Alexa Fluor 488 (1:500, S32354 lifetechnologies in PBS). Brain slices were washed three times for 30 min in PBS and mounted with Aqua-Poly/Mount. Filled neurons were scanned on a confocal microscope (Leica TCS SP8 SMD; LASX) and reconstructed from z-stacks (step size, 1-2 µM) using Fiji (imageJ).

2.4. Immunohistochemistry

After recording from feed-back interneurons, biocytin detection was performed as described above (section 1.3). However, slices were additionally stained for somatostatin (SST). After the final PBS wash, slices were treated with blocking solution

(3 % BSA in PBS-T (Triton X-100, 0.25 %) at room-temperature for two hours and then incubated with rabbit anti-SST antibody (1:500, T-4102, Peninsula Laboratories International in blocking solution) at 4 °C over night. On the next day, they were left at room-temperature for 30 min and afterwards washed with blocking solution three times for 10 min. Brain slices were incubated over night at 4 °C with donkey anti-rabbit Alexa fluor 647 (1:500, ab150075, Abcam in 3 % BSA in PBS-T 0.25 %) and on the next day washed three times in PBS for 10 min and mounted with Aqua-Poly/Mount.

2.5. Analysis of firing behavior in CA1 PCs and interneurons

For analysis of firing behavior, one-second-long current steps starting from -250 pA (∆50 pA) were injected in current-clamp mode. To investigate the maximum firing frequency, the current injection with the highest number of action potentials under control condition (ACSF) was compared to the equivalent current injection during S-Lic ((S)-Licarbazepin, 10,11-Dihydro-10-hydroxycarbamazepin) application. The baseline membrane potential was adjusted to -75 mV by continuous current injection for all measurements.

2.6. Analysis of feed-forward and feed-back inhibitory microcircuits

To stimulate feed-forward and feed-back inhibition in CA1 area, a stimulation electrode (Cluster electrode, FHC, controlled by isolated pulse stimulator, A-M Systems, model 2100) was used. Throughout all the recordings the same intracellular solution was used (see 2.2). This intracellular solution contained a low concentration of chloride and therefore results in a chloride reversal potential of -126 mV. Consequently, when holding the cell at -65 mV, the driving force for chloride to enter the cell is high. To record both feed-back and feed-forward inhibition in CA1 principal cells, IPSCs were recorded in the whole-cell voltage-clamp mode with a holding potential of -65 mV. To activate feed-back inhibition, CA1 axons were stimulated through a stimulation electrode placed into the alveus adjacent to the subiculum. This stimulation leads to antidromic activation of CA1 axons and recruitment of feedback inhibition. To prevent a direct monosynaptic excitation of inhibitory interneurons, a cut was made at the CA1/subiculum border through strata lacunosum moleculare, radiatum, pyramidale, and oriens, with only the alveus left intact (Pouille and Scanziani, 2004). A second cut was made at the CA1/CA3 border to limit spontaneous excitatory input to CA1 neurons (see **Figure 6**). To activate feed-forward inhibition, CA3 axons were stimulated by placing a stimulation electrode into the PC layer of CA3. To record EPSCs in either

feed-forward or feed-back interneurons, stimulation configuration remained the same as for stimulation of feed-forward and feed-back inhibition recorded in CA1 PCs. EPSCs were recorded in the whole-cell voltage-clamp mode with a holding potential of – 75 mV. The firing behavior of CA3 principal cells during activation of feed-forward microcircuits was examined with cell-attached recordings.

The following subsequent stimulation series was used to record either IPSCs or EPSCs: 50 Hz train of 25 stimuli, 20 Hz, 10 Hz, 5 Hz, 1 Hz with 2 stimuli and 100 Hz with 5 stimuli, each of the trains repeated 5 times with an interval of 15 seconds for the 50 Hz train and 10 seconds for all the other frequencies.

To isolate the GABAergic IPSCs recorded from pyramidal neurons unequivocally, the GABAA receptor antagonist gabazine (SR 95531 hydrobromide, 10 µM; Tocris) was applied at the end of feed-back stimulation experiments. Application of gabazine at the end of feed-forward stimulation was not feasible due to increased excitability of the recurrent excitatory CA3 network. During all stimulation experiments, the $GABA_B$ blocker CGP 52432 (500 nM; Tocris) was present in the bath solution.

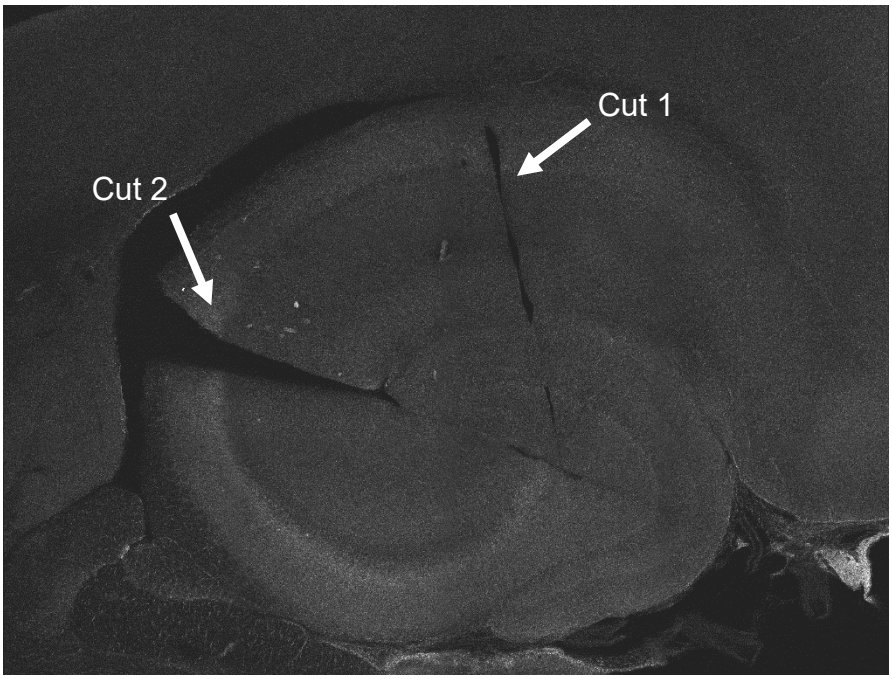

Figure 6: Manual cuts. Performed with scalpel. Cut 1 at the CA1/ subiculum border through strata lacunosum moleculare, radiatum, pyramidale and oriens with only the alveus left intact to prevent direct monosynaptic excitation of putative interneurons. Cut 2 at the CA1/CA3 border to limit spontaneous activity in CA1 neurons.

2.7. Selection criteria for interneurons

Two groups of interneurons were recorded in this work. The first group had somata in stratum radiatum of the CA1 area. These interneurons had a multipolar morphology with processes limited to stratum radiatum and stratum lacunosum moleculare, implying their preferential involvement in feed-forward, but not feed-back inhibitory circuits. The physiology of these stratum radiatum interneurons was characterized by their regular firing behavior, as well as feed-forward EPSCs that displayed pronounced depression upon repetitive stimulation (50 Hz). The second group of interneurons had a soma in stratum oriens of the CA1 area, and an axon targeting stratum lacunosum moleculare, thus corresponding to OLM neurons (Klausberger, 2009), which are strongly driven by excitation from CA1 neurons (Kullmann, 2011). These interneurons showed a regular firing pattern of up to 40 Hz and were driven by largely non-depressing EPSCs. We verified the identity of these cells by their expression of somatostatin in a subgroup of neurons (31 of 55 neurons).

2.8. Pharmacology

S-Lic was provided by BIAL Portela (BIA 2-194) and used at a concentration range also found in brain tissue from epilepsy patients (Rambeck et al., 2006). S-Lic (final concentration 100 µM and 300 µM) was dissolved in DMSO (dimethylsulfoxide). Therefore, ACSF contained the equivalent concentration of 0.1 % DMSO. Drug effects were analyzed 15 min after application start and washout was conducted for at least 15 min. The blocker IEM1460 (Tocris; final concentration 100 µM) was used to block CP-AMPAR (calcium permeable α-amino-3-hydroxy-5-methyl-4-isoxazolepropionic acid receptors) in feed-back interneurons.

2.9. Data analysis and statistics

Average values in the text and figures are shown as mean ± SEM. The properties of PSCs/PSPs were analyzed from an average of 5 sweeps (stimulus trains with 2–25 stimuli). Firing probabilities during the cell-attached recordings were calculated from 5 repetitions. Outliers were excluded if they exceeded two times standard deviation. Tests used for statistical analysis are indicated in the Results section.

3. Results

Contributions

Dr. Leonie Pothmann performed parts of the recordings testing the effects of 300 µM S-Lic on feed-back inhibition in CA1 of sham-control animals (**Figure 11C, E,** 5 of 8 cells). Data showing the effects of CBZ, PHT and LTG on feed-back inhibition in CA1 PCs (**Figure 11G**) were reanalyzed from Pothmann et al., 2014.

3.1. S-Lic effects on intrinsic firing properties of CA1 PCs

I first examined the classical effects of S-Lic on principal neuron firing (Holtkamp et al., 2018). Patch-clamp recordings were obtained from visually identified CA1 pyramidal neurons in sham-control and epileptic (post-SE) animals (see methods, **Figure 7**). Intrinsic firing was elicited with current injections, and the effects of either 100 or 300 µM S-Lic were tested (**Figure 7A, B**, example with 300 µM S-Lic). Neuronal firing was reduced with 300 µM S-Lic, both in sham-control and epileptic animals (**Figure 7C, D**, respectively). This manifested as a strong inhibition of maximal firing rates with 300 µM S-Lic. 100 µM of S-Lic had no significant effects on maximal firing rates in sham-control animals but affected maximal firing rates in post-SE animals (**Figure 7E,** RM two-way ANOVA using post-hoc Bonferroni's multiple comparison test for ACSF vs. S-Lic, for sham-control 100 µM, $p_{(1.255\ 14)}$=0.4597, 300 µM, $p_{(3.705\ 15)}$=0.0042, for post-SE 100 µM, $p_{(3.034\ 14)}$=0.0179, 300 µM, $p_{(3.155\ 15)}$=0.0131). To reveal use-dependent effects, I next quantified the reduction of firing rate during different time windows following onset of the current injections (**Figure 7C, D** lower panels). This analysis showed a weak dependence of blocking efficiency on the duration of the current injections. Thus, as expected, S-Lic inhibits firing of CA1 pyramidal neurons in a concentration-dependent manner in control and epileptic animals. Additionally, high-concentrations of S-Lic already affect firing during short cellular depolarization.

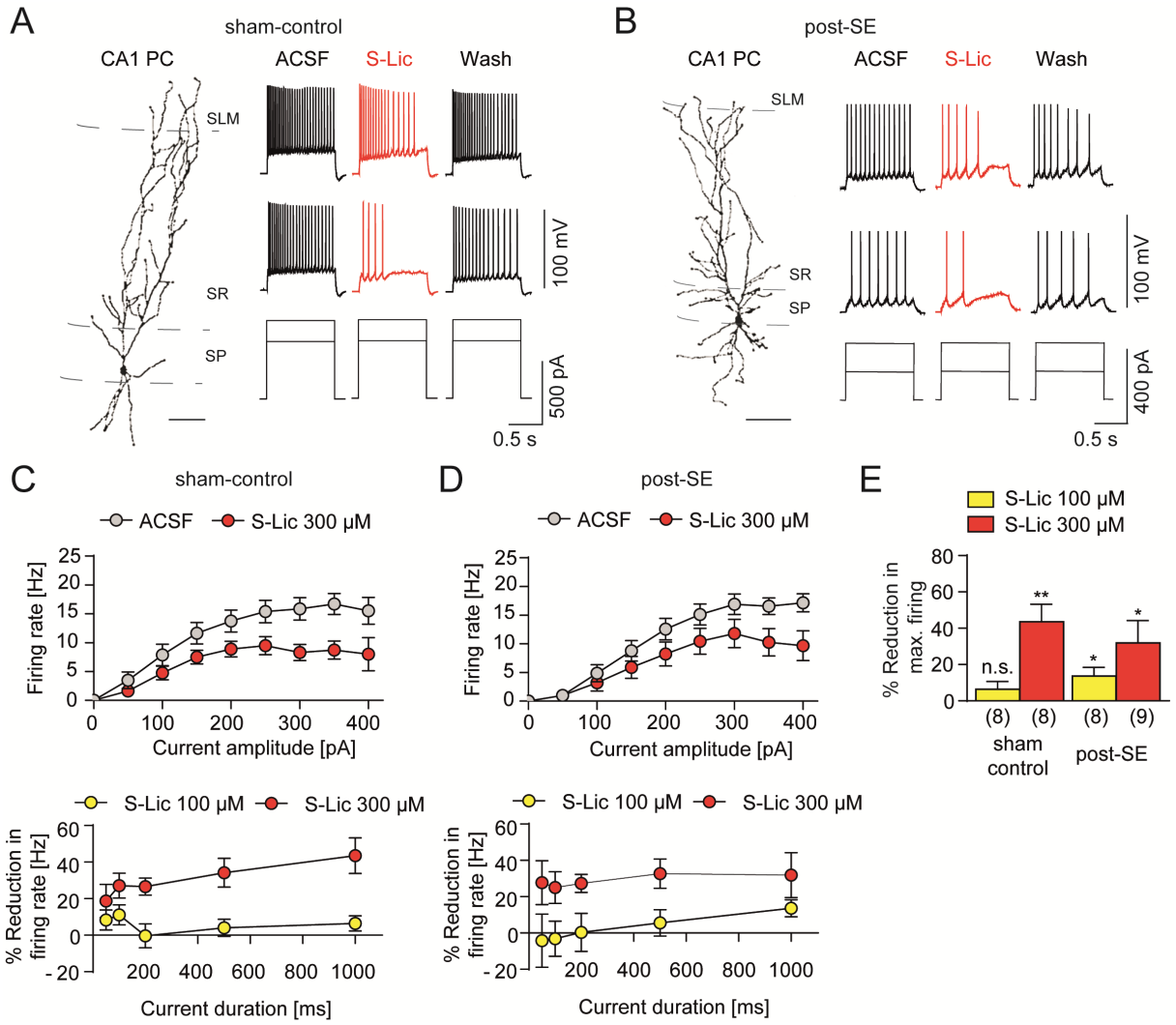

Figure 7: **S-Lic effects on firing properties of principal neurons.** ***A*** Left panel: Morphological reconstruction of a representative pyramidal neuron in sham-control animals. SP, Stratum pyramidale; SR, Stratum radiatum; SLM, Stratum lacunosum moleculare. Scale bar 100 µM. Right panel: Effects of 300 µM S-Lic on intrinsic firing induced by current injection (1000 ms). ***B*** Left panel: Morphological reconstruction of a representative pyramidal neuron in post-SE animals. Scale bar 100 µM. Right panel: Effects of 300 µM S-Lic on intrinsic firing induced by current injection (1000 ms). ***C, D*** Upper panel: Corresponding input-output relationship of the average firing rate during 1000 ms current injection versus the current amplitude for sham-control and post-SE animals respectively. Lower panel: Percent reduction in the firing rate during the first 50, 100, 200, 500 and 1000 ms of the current duration at maximum firing rate for 100 µM S-Lic (yellow circles) and 300 µM S-Lic (red circles) ***E*** Percent reduction of the maximal firing rate by 100 µM and 300 µM S-Lic in sham-control and post-SE animals. * and ** indicate $p<0.05$ and 0.01 respectively and n.s. indicates $p>0.05$ for RM two-way ANOVA using Bonferroni's multiple comparison test. n numbers indicated in parentheses.

This dataset also allowed me to compare the properties of control and epileptic CA1 pyramidal neurons. However, I did not find any differences in passive and active membrane properties between sham-control and post-SE animals (**Table 1,** for absolute values see **Table 4** in appendix).

I also quantified the effects of S-Lic on active and passive properties of pyramidal neurons. I found that S-Lic reduces sag ratio for both concentrations in pyramidal neurons. 100 µM but not 300 µM S-Lic affected AHP delay and AP threshold (**Table 1**).

Table 1: Effects of S-Lic on active and passive properties of pyramidal neurons. Rm: membrane resistance, tau: membrane time constant, Cm: membrane capacitance, Sag ratio: % reduction of hyperpolarization by h-current during a -100 pA current step, mAHP: medium after hyperpolarization, AHP delay: time of afterhyperpolarization after peak, Threshold: action potential threshold, max. dV/dt: maximal action potential slope, Half width: action potential width at half-maximal amplitude between threshold and peak. Two-way ANOVA of ACSF vs. 300 µM or 100 µM S-Lic, p-values are considered significant after Bonferroni correction with $p<0.0055$.

	300 µM			100 µM		
R_m (MOhm)	Interaction	F=3.809	P=0.0687	Interaction	F=0.6377	P=0.4379
	S-Lic	F=4.118	P=0.0594	S-Lic	F=0.04468	P=0.8356
	Epilepsy	F=3.042	P=0.1003	Epilepsy	F=1.969	P=0.1824
tau (ms)	Interaction	F=0.5501	P=0.4690	Interaction	F=0.1042	P=0.7516
	S-Lic	F=1.197	P=0.2901	S-Lic	F=0.4221	P=0.5264
	Epilepsy	F=1.328	P=0.2660	Epilepsy	F=1.648	P=0.2201
C_m (pF)	Interaction	F=2.542	P=0.1304	Interaction	F=1.455	P=0.2477
	S-Lic	F=4.663	P=0.0464	S-Lic	F=0.6573	P=0.4311
	Epilepsy	F=0.1802	P=0.6769	Epilepsy	F=0.01198	P=0.9144
Sag ratio	Interaction	F=0.8894	P=0.3597	Interaction	F=2.118	P=0.1676
	S-Lic	F=24.92	P=0.0001*	S-Lic	F=15.53	P=0.0015*
	Epilepsy	F=9.257	P=0.0078	Epilepsy	F=0.4609	P=0.5083
mAHP amplitude (mV)	Interaction	F=0.8901	P=0.3595	Interaction	F=1.903	P=0.1894
	S-Lic	F=8.934	P=0.0087	S-Lic	F=5.072	P=0.0409
	Epilepsy	F=4.505	P=0.0498	Epilepsy	F=3.029	P=0.1037
AHP delay (ms)	Interaction	F=1.047	P=0.3214	Interaction	F=1.41	P=0.2548
	S-Lic	F=5.958	P=0.0267	S-Lic	F=12.16	P=0.0036*
	Epilepsy	F=0.08168	P=0.7787	Epilepsy	F=0.2909	P=0.5981
Threshold (mV)	Interaction	F=1.074	P=0.3155	Interaction	F=1.507	P=0.2398
	S-Lic	F=1.722	P=0.2079	S-Lic	F=27.52	P=0.0001*
	Epilepsy	F=0.2818	P=0.6028	Epilepsy	F=0.3098	P=0.5866
max. dV/dt (V/s)	Interaction	F=0.4038	P=0.5341	Interaction	F=0.01854	P=0.8936
	S-Lic	F=25.29	P=0.0001	S-Lic	F=1.67	P=0.2171
	Epilepsy	F=3.024	P=0.1012	Epilepsy	F=0.6186	P=0.4447
Half width (ms)	Interaction	F=3.477	P=0.0807	Interaction	F=0.0501	P=0.8261
	S-Lic	F=0.6939	P=0.4171	S-Lic	F=0.4388	P=0.5185
	Epilepsy	F=5.171	P=0.0371	Epilepsy	F=2.148	P=0.1648

3.2. S-Lic effects on feed-forward inhibition in CA1

To investigate the effects of S-Lic on inhibition in the brain, I studied the canonical inhibitory motifs in hippocampal CA1. The two main inhibitory motifs in this region are feed-forward and feed-back inhibition. To record feed-forward inhibition I stimulated with a bipolar stimulation electrode within the CA3 PC layer (**Figure 8A**) and recorded feed-forward inhibitory post-synaptic currents (FF-IPSCs) in CA1 pyramidal neurons. FF-IPSCs show a strong depression during a 50 Hz train stimulation in both sham-control and epileptic animals (**Figure 8B**). Interestingly, washin of high concentrations of S-Lic (300 µM) reduced peak amplitudes of FF-IPSCs in sham-control and epileptic animals (**Figure 8C, D**). I quantified the effects of S-Lic on the first IPSCs during the 50 Hz train stimulation and found large effects on FF-IPSCs for 300 µM S-Lic in both sham-control and epileptic animals (**Figure 8E,** RM two-way ANOVA using post-hoc Bonferroni's multiple comparison test for ACSF vs. S-Lic, 48.19 ± 10.06 % reduction in sham-control, $p_{(5.684\ 14)}$=0.0001; and 78.26 ± 4.19 % reduction in post-SE, ACSF vs. S-Lic, $p_{(8.143\ 14)}$<0.0001). The outcome of the treatment of 300 µM S-Lic on FF-IPSCs also depends on the pathology of the animal, shown by significant interaction of the groups (RM two-way ANOVA, interaction F(1, 14)=5.51, p=0.0341, pathology F(1, 14)=5.491, p=0.0344). However, lower concentrations of S-Lic like 100 µM did not affect IPSC amplitudes significantly either in sham-control or epileptic animals (**Figure 8E**, yellow bars, RM two-way ANOVA using post-hoc Bonferroni's multiple comparison test for ACSF vs. S-Lic, sham-control, $p_{(0.2183\ 16)}$>0.9999 and post-SE, $p_{(0.03921\ 16)}$>0.9999). Additionally, I investigated the effect on last FF-IPSCs during the 50 Hz train. To this end I compared the average of the last three FF-IPSCs but found only a significant reduction in sham-control, but not in epileptic animals (**Figure 8F,** RM two-way ANOVA using post-hoc Bonferroni's multiple comparison test for ACSF vs. S-Lic, sham-control: 100 µM $p_{(3.225\ 16)}$=0.0106, 300 µM $p_{(6.572\ 14)}$<0.0001, post-SE 100 µM $p_{(0.1564\ 16)}$>0.9999, 300 µM $p_{(0.6249\ 14)}$>0.9999).

The reduction in FF-IPSCs amplitude could be due to a weaker stimulation of CA3 axons during the washin of high concentrations of S-Lic. To investigate this possibility, I again electrically stimulated within the CA3 pyramidal layer, but this time recorded action potential firing in the cell-attached mode from CA3 PCs (**Figure 8G**). Neither in sham-control nor in epileptic animals I found any effect of 300 µM S-Lic on synaptically evoked action potentials in CA3 neurons (**Figure 8H, I**). These results suggest that axon stimulation of CA3 PCs is unaffected by S-Lic. Still I could show that high concentrations of S-Lic reduce feed-forward inhibition recorded in CA1 PCs.

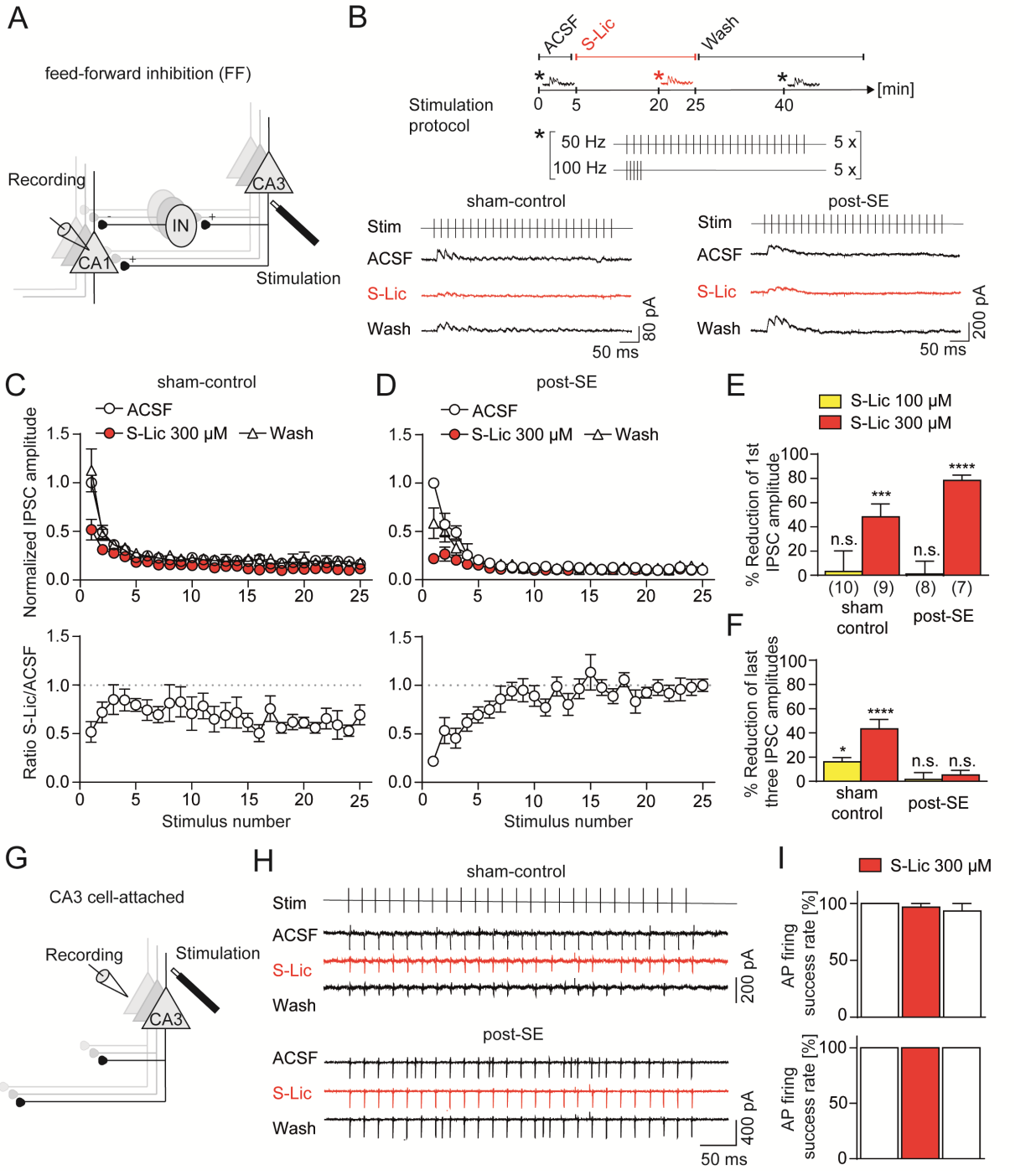

Figure 8: S-Lic effects on feed-forward inhibition. ***A*** Recording configuration to elicit feed-forward inhibition in CA1 pyramidal neurons. ***B*** Stimulation protocol used with bipolar electrode using 50 Hz and 100 Hz trains (upper panel), representative recordings of feed-forward IPSCs with application of 300 µM S-Lic and washout of S-Lic for sham-control and post-SE animals. ***C, D*** Corresponding S-Lic effects on peak IPSC amplitudes during 50 Hz stimulation for sham-control and post-SE animals, respectively. Upper panels show IPSC amplitudes normalized to first stimulus in ACSF. Lower panels show the ratio of FF-IPSC amplitudes recorded during ACSF and S-Lic. ***E, F*** Percent reduction in the first IPSC amplitude and last three IPSC amplitudes respectively for 100 µM and 300 µM S-Lic for sham-control and post-SE animals. ***G*** Recording configuration to elicit antidromic stimulation of CA3 PCs.

3.3. No effects of S-Lic on activation of feed-forward interneurons

Another explanation of reduced feed-forward inhibition in CA1 PCs during washin of S-Lic could be that activation of involved feed-forward interneurons is affected by S-Lic. To test this, I recorded from putative feed-forward interneurons (soma in stratum radiatum of CA1 area) and stimulated Schaffer collaterals in CA3 pyramidal layer at 50 Hz and 100 Hz (**Figure 9C left panel**). All interneurons showed a multipolar morphology (see methods for selection criteria, representative interneuron morphology in **Figure 9B**). The recorded EPSCs in putative feed-forward interneurons showed depression during 50 Hz stimulation trains both in sham-control and epileptic animals (**Figure 9C**, right panels). Both washin of 300 µM or 100 µM S-Lic did not have any effects on EPSC amplitudes. I quantified the change of the first EPSC amplitude by S-Lic and did not find any significant effects for both sham-control and epileptic animals (**Figure 9D-F,** RM two-way ANOVA using post-hoc Bonferroni's multiple comparison test for ACSF vs. S-Lic, sham-control: 100 µM $p_{(1.869\ 16)}$=0.1600, 300 µM $p_{(2.411\ 10)}$=0.0732, post-SE 100 µM $p_{(1.696\ 16)}$=0.2184, 300 µM $p_{(0.395\ 10)}$>0.9999). These results suggest that reduced feed-forward inhibition during washin of S-Lic are not due to effects on Schaffer collateral mediated excitation of interneurons.

Figure 8 continuum: ***H*** Representative cell-attached recordings of CA3 action potentials with application of 300 µM S-Lic and washout of S-Lic for sham-control (upper panel) and post-SE animals (lower panel). ***I*** Percent action potential firing success rate before, during and after washout of 300 µM S-Lic. *, *** and **** indicate p<0.05, 0.001 and 0.0001 respectively and n.s. indicates p>0.05 for RM two-way ANOVA using Bonferroni's multiple comparison test. n numbers indicated in parentheses.

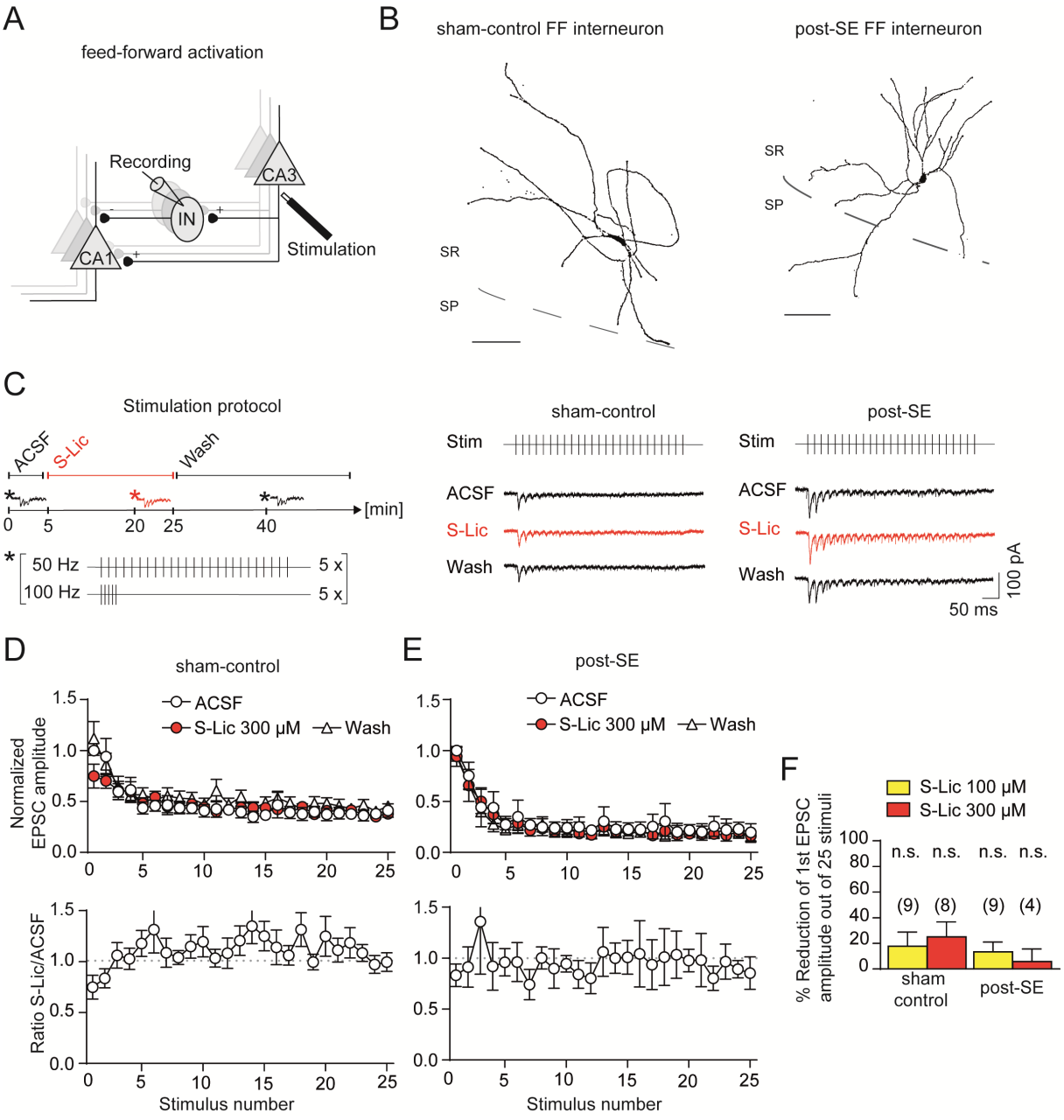

Figure 9: Dissection of S-Lic effects on activation of feed-forward interneurons ***A*** Recording configuration to elicit feed-forward activation in CA1 feed-forward interneurons. ***B*** Morphological reconstruction of representative feed-forward interneurons in sham-control and post-SE animals respectively. SP, Stratum pyramidale and SR, Stratum radiatum. Scale bar 100 µM. ***C*** Stimulation protocol used with bipolar electrode using 50 Hz and 100 Hz trains (left panel), representative recordings of feed-forward EPSCs with application of 300 µM S-Lic and washout of S-Lic for sham-control and post-SE animals (right panels). ***D, E*** Corresponding S-Lic effects on peak EPSC amplitudes during 50 Hz stimulation for sham-control and post-SE animals respectively. EPSC amplitudes normalized to first stimulus in ACSF (upper panels). Ratio of ACSF and S-Lic for sham-control and post-SE, respectively (lower panels). ***F*** Percent reduction in the first EPSC amplitude respectively for 100 µM and 300 µM S-Lic for sham-control and post-SE animals. n.s. indicates $p>0.05$ for RM two-way ANOVA using Bonferroni's multiple comparison test. n numbers indicated in parentheses.

3.4. S-Lic effects on intrinsic firing properties of feed-forward interneurons

Reduction in feed-forward inhibition due to washin of S-Lic could be also explained by an effect on active or passive properties of putative feed-forward interneurons due to application of S-Lic. To investigate effects of S-Lic on feed-forward interneurons I performed step current injections and recorded the voltage response for hyperpolarizing and depolarizing current injections. I did not find any significant difference during washin of either 100 µM or 300 µM S-Lic in sham-control or epileptic animals (**Table 2**).

Next I analyzed the effects of S-Lic on repetitive firing. Putative feed-forward interneurons showed regular firing patterns of around 50 Hz (representative examples in **Figure 10A, B**). I found that 300 µM S-Lic inhibited firing only in epileptic animals. An analysis of the reduction in firing rate for different time windows of the action potential train revealed that 300 µM S-Lic blocks firing in a use-dependent manner (**Figure 10C,D lower panels**). Additionally, the maximum firing was not affected by 100 µM S-Lic for both sham-control and epileptic animals (**Figure 10E,** RM two-way ANOVA using post-hoc Bonferroni's multiple comparison test for ACSF vs. 300 µM S-Lic, sham control: 29.4±8.0 %, $p_{(2.428\ 13)}$=0.0608, post-SE: 44,6 ± 9.0 %, $p_{(3.721\ 13)}$=0.0051, and RM two-way ANOVA using post-hoc Bonferroni's multiple comparison test for ACSF vs. 100 µM S-Lic, sham control: 11.5±5.8 %, $p_{(0.5059\ 13)}$>0.9999, post-SE: 13.8 ± 10.4 %, $p_{(1.672\ 13)}$=0.2368).

Additionally, I compared active and passive properties of stratum radiatum interneurons between sham-control and epileptic animals. However, I did not find any significant differences between these two groups (**Table 2,** for absolute values see **Table 4** in appendix).

Collectively, these results show that feed-forward inhibition in epileptic animals is significantly reduced by high concentrations (300 µM) of S-Lic, most likely via reduced intrinsic firing of interneurons contributing to feed-forward inhibition.

Table 2: Effects of S-Lic on active and passive properties of stratum radiatum interneurons. R_m: membrane resistance, tau: membrane time constant, C_m: membrane capacitance, Sag ratio: % reduction of hyperpolarization by h-current during a -100 pA current step, mAHP: medium after hyperpolarization, AHP delay: time of afterhyperpolarization after peak, Threshold: action potential threshold, max. dV/dt: maximal action potential slope, Half width: action potential width at half-maximal amplitude between threshold and peak. Two-way ANOVA, p-values are considered significant after Bonferroni correction with p<0.0055.

	300 µM			100 µM		
R_m (MOhm)	Interaction	F=3.406	P=0.0879	Interaction	F=0.01135	P=0.9168
	S-Lic	F=2.38	P=0.1469	S-Lic	F=0.1168	P=0.7380
	Epilepsy	F=0.1882	P=0.6715	Epilepsy	F=0.1608	P=0.6950
tau (ms)	Interaction	F=1.372	P=0.2624	Interaction	F=0.7582	P=0.3997
	S-Lic	F=3.227	P=0.0957	S-Lic	F=3.658	P=0.0781
	Epilepsy	F=1.505	P=0.2417	Epilepsy	F=0.2073	P=0.6564
C_m (pF)	Interaction	F=0.9995	P=0.3357	Interaction	F=2.395	P=0.1457
	S-Lic	F=1.324	P=0.2706	S-Lic	F=4.779	P=0.0477
	Epilepsy	F=2.815	P=0.1173	Epilepsy	F=0.8164	P=0.3827
Sag ratio	Interaction	F=10.44	P=0.0066	Interaction	F=4.388	P=0.0564
	S-Lic	F=6.827	P=0.0215	S-Lic	F=3.479	P=0.0849
	Epilepsy	F=3.545	P=0.0823	Epilepsy	F=0.9096	P=0.3576
mAHP amplitude (mV)	Interaction	F=0.1749	P=0.6826	Interaction	F=1.943	P=0.1867
	S-Lic	F=3.382	P=0.0888	S-Lic	F=2.085	P=0.1724
	Epilepsy	F=0.02812	P=0.8694	Epilepsy	F=2.524	P=0.1362
AHP delay (ms)	Interaction	F=3.193	P=0.0973	Interaction	F=0.6525	P=0.4338
	S-Lic	F=1.284	P=0.2776	S-Lic	F=1.9	P=0.1913
	Epilepsy	F=0.7537	P=0.4011	Epilepsy	F=0.218	P=0.6483
Threshold (mV)	Interaction	F=3.033	P=0.1052	Interaction	F=0.1561	P=0.6992
	S-Lic	F=1.031	P=0.3284	S-Lic	F=0.1915	P=0.6689
	Epilepsy	F=2.632	P=0.1287	Epilepsy	F=0.03977	P=0.8450
max. dV/dt (V/s)	Interaction	F=1.011	P=0.3329	Interaction	F=0.52	P=0.4836
	S-Lic	F=2.37	P=0.1477	S-Lic	F=2.143	P=0.1670
	Epilepsy	F=3.241	P=0.0951	Epilepsy	F=0.9576	P=0.3456
Half width (ms)	Interaction	F=5.038e-005	P=0.9944	Interaction	F=0.03103	P=0.8629
	S-Lic	F=2.144	P=0.1669	S-Lic	F=2.083	P=0.1726
	Epilepsy	F=0.8736	P=0.3670	Epilepsy	F=2.136	P=0.1676

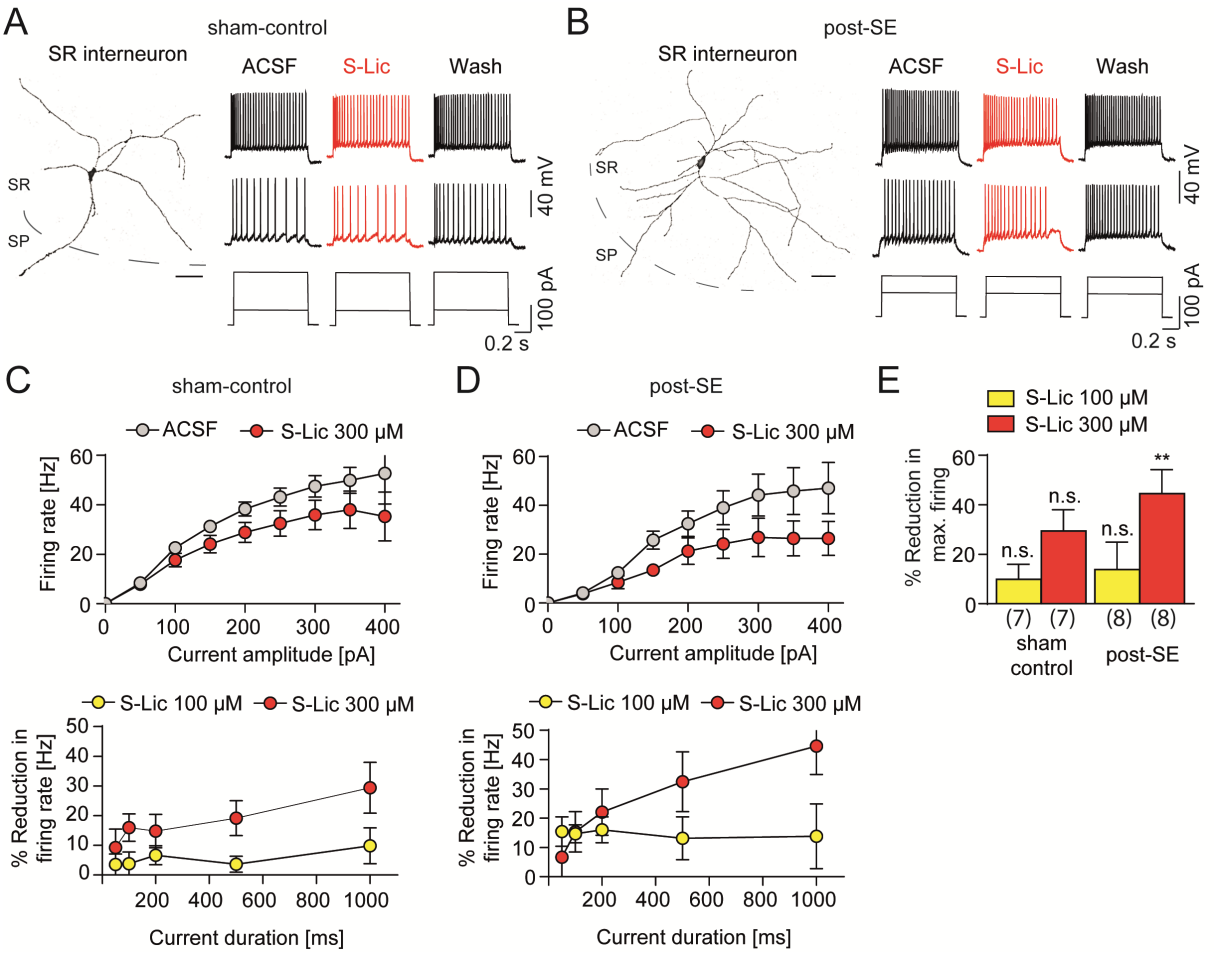

Figure 10: S-Lic effects on firing properties of feed-forward interneurons. ***A*** Left panel: Morphological reconstruction of a representative feed-forward interneuron in sham-control animals. SP, Stratum pyramidale; SR, Stratum radiatum. Scale bar 100 µM. Right panel: Effects of 300 µM S-Lic on intrinsic firing induced by current injection (1000 ms). ***B*** Left panel: Morphological reconstruction of a representative feed-forward interneuron in post-SE animals. Scale bar 100 µM. Right panel: Effects of 300 µM S-Lic on intrinsic firing induced by current amplitude (1000 ms). ***C, D*** Corresponding input-output relationship of the average firing rate during 1000 ms current injection versus the current amplitude for sham-control and post-SE animals respectively (upper panels). Corresponding relationship of the percent reduction in firing rate during 50, 100, 200 and 1000 ms current duration for current amplitude with maximum firing rate during ACSF and corresponding S-Lic condition for sham-control and post-SE animals respectively (lower panels). ***E*** Percent reduction in the maximal firing rate for 100 µM and 300 µM S-Lic for sham-control and post-SE animals. ** indicates $p<0.01$ and n.s. indicates $p>0.05$ for RM two-way ANOVA using Bonferroni's multiple comparison test. n numbers indicated in parentheses.

3.5. S-Lic effects on feed-back inhibition

The second important inhibitory motif in the hippocampus is the feed-back inhibition. Does S-Lic also reduce inhibition in this motif, like it does for feed-forward inhibition? To test this, I evoked feed-back inhibition in CA1 PCs via electrical stimulation of CA1 PC axons within the alveus. Stimulation was carried out with 50 Hz and 100 Hz stimulation trains as used to probe feed-forward inhibition, while recording feed-back IPSCs in CA1 PCs (**Figure 11A**). Similar to FF-IPSCs, feed-back IPSCs also depressed during the stimulation train (**Figure 11B**). S-Lic does not seem to affect feed-back inhibition in healthy animals. However, when I compared IPSC amplitudes in epileptic animals, I could observe a consistent and large increase in feed-back IPSCs after washout of S-Lic (increase to 175.6 ± 28.9 % of the ACSF value, n=10, see triangles in **Figure 11D,** and quantification in **Figure 11F,** RM two-way ANOVA using post-hoc Bonferroni's multiple comparison test for ACSF vs. wash, post-SE $p_{(3.475\ 16)}$=0.0062, sham-control $p_{(0.2831\ 16)}$>0.9999).

To exclude whether this potentiation is just dependent on my constant stimulation over time, I stimulated as before but did not washin S-Lic but ACSF. I could not observe any significant changes in IPSC amplitude and no potentiation (**Figure 11G**, RM two-way ANOVA using post-hoc Bonferroni's multiple comparison test for ACSF vs. Wash $p_{(1.653\ 20)}$=0.4558). Next I wanted to investigate, whether this effect of potentiation is specific for the AED S-Lic as compared to other AEDs? For this purpose I reanalyzed data from Pothmann et al. 2014, where they tested the effects of CBZ, PHT and lamotrigine (LTG) on feed-back inhibition. The application of these AEDs did not result in IPSC potentiation (**Figure 11G,** 30 µM, 25 µM and 50 µM, respectively RM two-way ANOVA using post-hoc Bonferroni's multiple comparison test for ACSF vs. Wash, for CBZ $p_{(1.806\ 20)}$=0.3437, for LTG $p_{(0.579\ 20)}$>0.9999, for PHT $p_{(0.7347\ 20)}$>0.9999). This raises the possibility that even though S-Lic significantly decreases feed-forward inhibition, it after washout leads to a very pronounced, sustained increase in feed-back inhibition. I term this increase AED-evoked plasticity of inhibition.

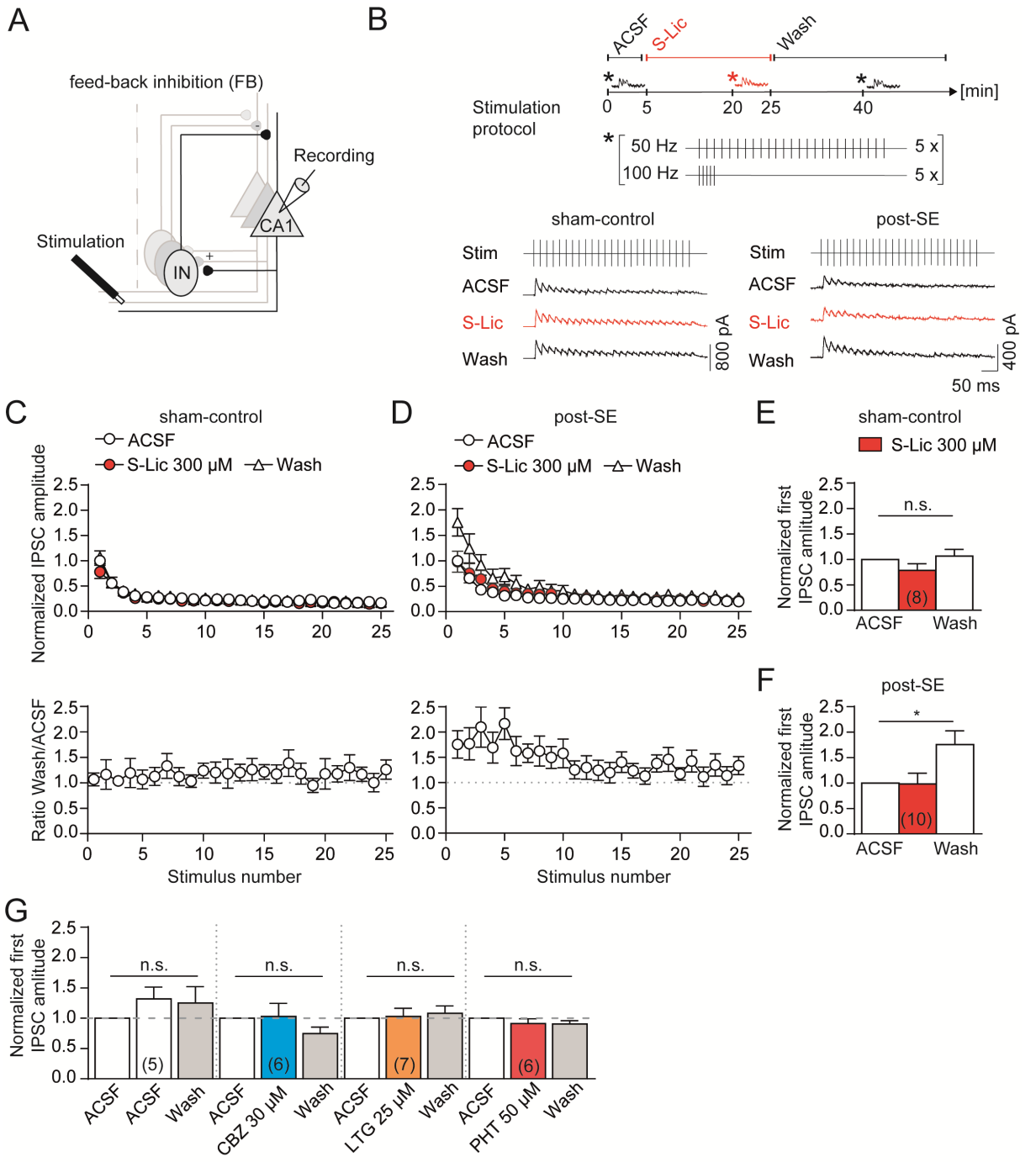

Figure 11: S-Lic effects on feed-back inhibition. ***A*** Recording configuration to elicit feed-back inhibition in CA1 pyramidal neurons. ***B*** Stimulation protocol used with bipolar electrode using 50 Hz and 100 Hz trains (upper panel), representative recordings of feed-back IPSCs with application of 300 µM S-Lic and washout of S-Lic for sham-control and post-SE animals. ***C, D*** Corresponding S-Lic effects on peak IPSC amplitudes during 50 Hz stimulation for sham-control and post-SE animals respectively. Upper panels show IPSC amplitudes normalized to first stimulus in ACSF. Lower panels show the ratio of ACSF and S-Lic. ***E, F*** First IPSC amplitude normalized to first stimulus in ACSF with washin and washout of 300 µM S-Lic for sham-control and post-SE animals. ***G*** First IPSC amplitude normalized to first stimulus in ACSF with washin and washout of either ACSF, CBZ 30 µM, LTG 25 µM or PHT 50 µM. CBZ. LTP and PHT data reanalyzed from Pothmann et al. 2014. * indicates $p<0.05$ and n.s. indicates $p>0.05$ for RM two-way ANOVA using Bonferroni's multiple comparison test. n numbers indicated in parentheses.

3.6. S-Lic effects and CP-AMPAR

Interestingly, putative feed-back interneurons like OLMs show a so called anti-Hebbian LTP (Lamsa et al., 2007a). In contrast to Hebbian LTP which depends on NMDARs and a depolarized postsynapse, anti-Hebbian LTP is evoked by CP-AMPAR and a hyperpolarized postsynapse. CP-AMPARs lack the GluR2 subunit and this subunit makes the channel permeable to Ca^{2+}. Additionally, these channels are blocked by cellular depolarization due to polyamines like spermine, which occlude the channel pore. So far, this anti-Hebbian LTP has been only shown in interneurons selective to the feed-back pathway and not in other types of interneurons or principal cells in the hippocampus (Lamsa et al., 2007a; Szabo et al., 2012).

If the observed AED-evoked plasticity depends on CP-AMPAR, it should be prevented by specific inhibitors of these receptors. Therefore, I recorded feed-back IPSCs (**Figure 12A**) and applied either the CP-AMPA receptor blocker IEM1460 together with or instead of S-Lic in slices from epileptic animals (**Figure 12B**). During both conditions, I was able to observe a reduced IPSC amplitude during the washin of either S-Lic with IEM1460 or IEM1460 alone (**Figure 12C**). This observation suggests that feed-back inhibition stimulated via the alveus is indeed dependent on the activation of CP-AMPAR. More importantly, plasticity of inhibition was no longer observed after washout of IEM1460 (**Figure 12C,** RM two-way ANOVA using post-hoc Bonferroni's multiple comparison test for ACSF vs. Wash for washin of S-Lic and IEM n=6, $p_{(0.4295\ 10)}$>0.9999, for washin of IEM n=7, $p_{(0.1076\ 10)}$>0.9999). These results show that the observed AED-evoked plasticity depends on Ca^{2+}-permeable AMPARs.

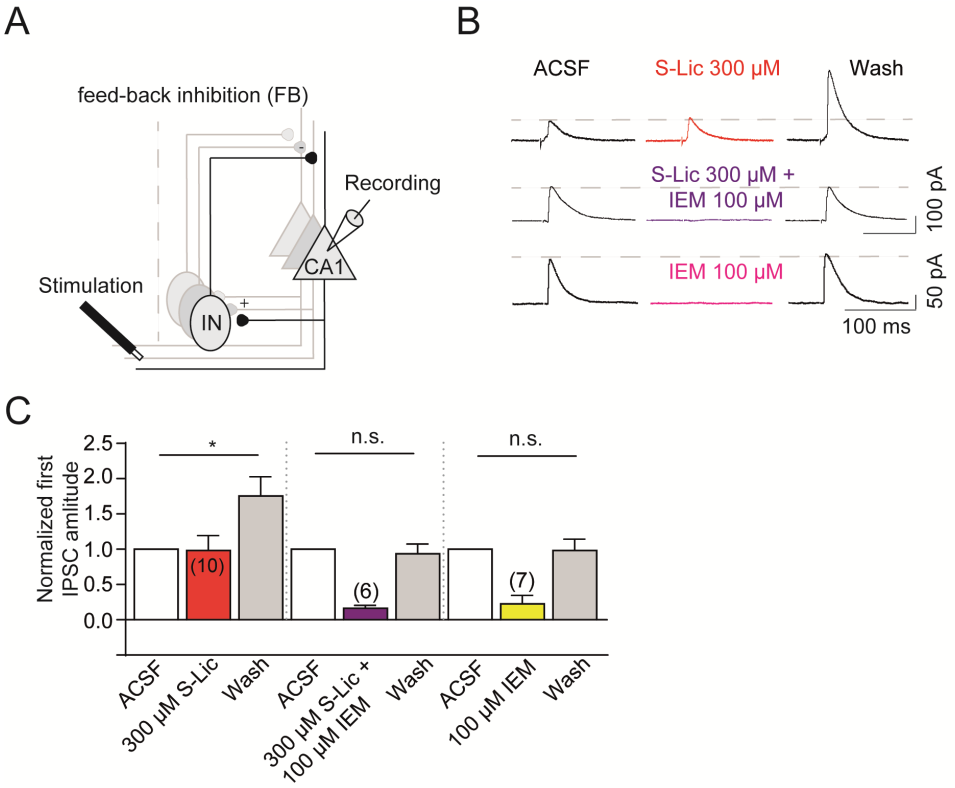

Figure 12: S-Lic effects and CP-AMPARs. ***A*** Recording configuration to elicit feed-back inhibition in CA1 pyramidal neurons. ***B*** Representative recordings of feed-back IPSCs with application of and washout for either 300 µM S-Lic, 300 µM S-Lic and 100 µM IEM1460 or 100 µM IEM1460 for post-SE animals. ***C*** First IPSC amplitude normalized to first stimulus in ACSF with washin and washout of either 300 µM S-Lic (left group of bar graphs already presented in Figure 11 F, but shown here for comparison), 300 µM S-Lic and 100 µM IEM1460 or 100 µM IEM1460 for post-SE animals. n.s. indicates p>0.05 for RM two-way ANOVA using Bonferroni's multiple comparison test. n numbers indicated in parentheses.

Previous studies have shown that expression of CP-AMPARs increases after SE, due to down-regulation of GluR2 subunits (Friedman et al., 1994; Oguro et al., 1999; Grooms et al., 2000; Prince et al., 2000; Sommer et al., 2001). To investigate whether an upregulation of CP-AMPARs takes place after SE I used the specific blocker IEM1460, to compare EPSCs in Ca^{2+}-permeable AMPARs expressing feed-back interneurons. I recorded from interneurons with their soma in stratum oriens, which showed potentiated EPSCs (**Figure 13C**, Pouille and Scanziani, 2004a). Additionally, I confirmed the identity of recorded interneurons as OLMs by immunostaining for somatostatin (**Figure 13B** sham-control (upper panel) and post-SE (lower panel)). I stimulated feed-back excitation (**Figure 13A**) and determined the effects of IEM1460 on the magnitude of AMPAR mediated EPSCs. IEM1460 potently blocked feed-back EPSCs to a similar extent in both sham-control and post-SE animals (**Figure 13D-F,**

RM two-way ANOVA using post-hoc Bonferroni's multiple comparison test for sham-control 69.3±4.7 %, n=6, $p_{(2.881\ 11)}$=0.0299, and for post-SE 68.4±8.8 %, n=7, $p_{(2.907\ 11)}$=0.0285, comparison between sham-control and post-SE using RM two-way ANOVA, F(1, 11)=0.1594 p=0.6973). This indicates that up-regulation of CP-AMPARs cannot account for the fact that AED-evoked potentiation occurs in epileptic, but not in control animals.

Another set of studies has shown that intracellular polyamines like spermine, which block CP-AMPARs in a voltage-dependent manner (Bowie and Mayer, 1995; Kamboj et al., 1995; Rozov and Burnashev, 1999), are reduced in chronic epilepsy (Royeck et al., 2015). This potentially results in increased availability of CP-AMPARs, which could be one potential explanation why I observe AED-induced plasticity only in epileptic animals. In whole cell recordings, washout of intracellular polyamines occurs gradually after formation of whole-cell mode, and leads to increases in synaptic responses mediated by CP-AMPARs, as well as changes in paired-pulse properties (Rozov and Burnashev, 1999). In both sham-control and epileptic rats, I observed an up-regulation of CP-AMPA responses elicited by feed-back circuit stimulation over the first 10 minutes of whole-cell recording. The magnitude of this up-regulation was variable, but not significantly different between sham-control and epileptic rats (**Figure 13G,** sham-control: 1.88±0.16 % and post-SE: 3.63±0.76 %, comparison between sham-control and post-SE using RM two-way ANOVA F(1, 11)=3.865 p=0.0751). Therefore, an equivalent concentration of intracellular polyamines in sham-control and post-SE animals cannot account for the observed AED-evoked plasticity in epileptic animals.

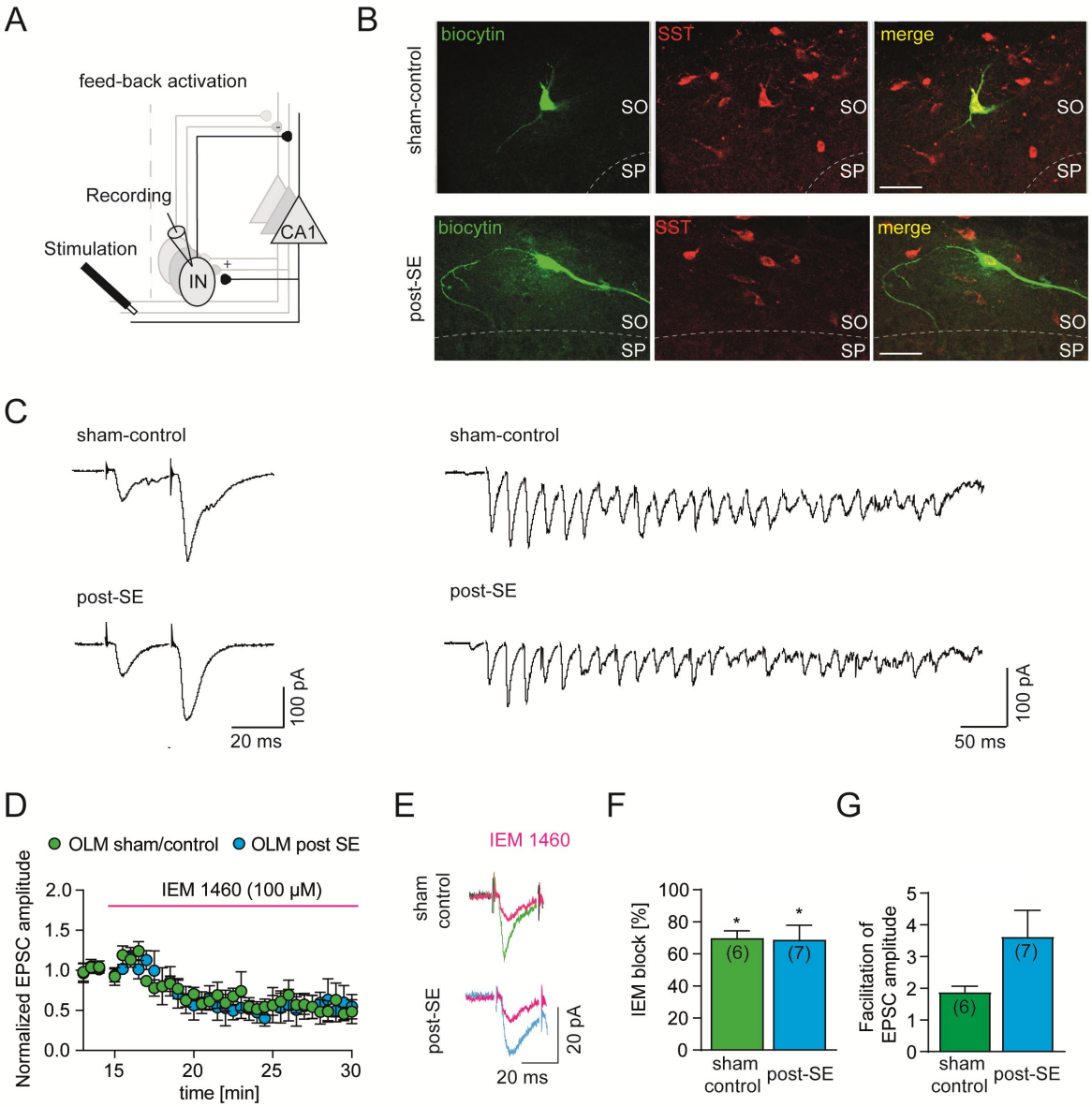

Figure 13: S-Lic effects on CP-AMPARs in feed-back interneurons. ***A*** Recording configuration to elicit feed-back activation in CA1 feed-back interneurons. ***B*** Biocytin reconstructed cell (left) with somatostatin staining (middle) and merged images (right), upper panel sham-control, lower panel post-SE. Scale bars 50 µM. ***C*** Representative recordings of feed-back activation of putative OLM interneurons with potentiated EPSC amplitudes, left paired pulse, right 50 Hz train with 25 stimuli. ***D*** EPSC amplitudes over a time period of 30 min normalized to last three EPSC amplitudes with application of 100 µM IEM1460 in sham-control (green circles) and post-SE (blue circles) animals. ***E*** Representative recordings of feed-back EPSCs with application of 100 µM IEM for sham-control and post-SE animals respectively. ***F*** IEM block calculated by the percent difference between the maximum EPSC amplitude before application of 100 µM IEM1460 and the average of the last five EPSC amplitudes blocked by IEM1460 and for sham-control and post-SE animals. ***G*** Facilitation of EPSC amplitude calculated by the normalized increase of EPSC amplitude of first stimulation to maximal EPSC amplitude for sham-control and post-SE animals. * indicates $p<0.05$ for RM two-way ANOVA using Bonferroni's multiple comparison test. n numbers indicated in parentheses.

3.7. S-Lic effects on activation of feed-back interneurons

Next I examined if 300 µM S-Lic affects feed-back activation of putative feed-back interneurons. I evoked feed-back activation with the bipolar stimulation configuration in the alveus of CA1 and recorded from interneurons with their soma in stratum oriens, which presumably mediate feed-back inhibition to the distal dendrites of CA1 PCs (stimulation configuration in **Figure 14A**). Feed-back EPSCs elicited by alveus stimulation showed facilitation during 50 Hz stimulation trains in both sham-control and epileptic animals (representative examples in **Figure 14B**). Both in sham-control and post-SE animals, I did not observe any effects of S-Lic on the average EPSC amplitude during 50 Hz train stimulation (**Figure 14C,** RM two-way ANOVA using post-hoc Bonferroni's multiple comparison test for ACSF vs. S-Lic for sham-control 24.1±5.0 %, $p_{(1.551\ 12)}$=0.2936, for post-SE 8.6±10.8 %, $p_{(0.8111\ 12)}$=0.8662). These results show that, S-Lic does not change the AMPAR-mediated synaptic drive of feed-back interneurons in post-SE animals and thereby cannot explain the AED-induced plasticity induced by S-Lic only in epileptic and not in sham-control animals.

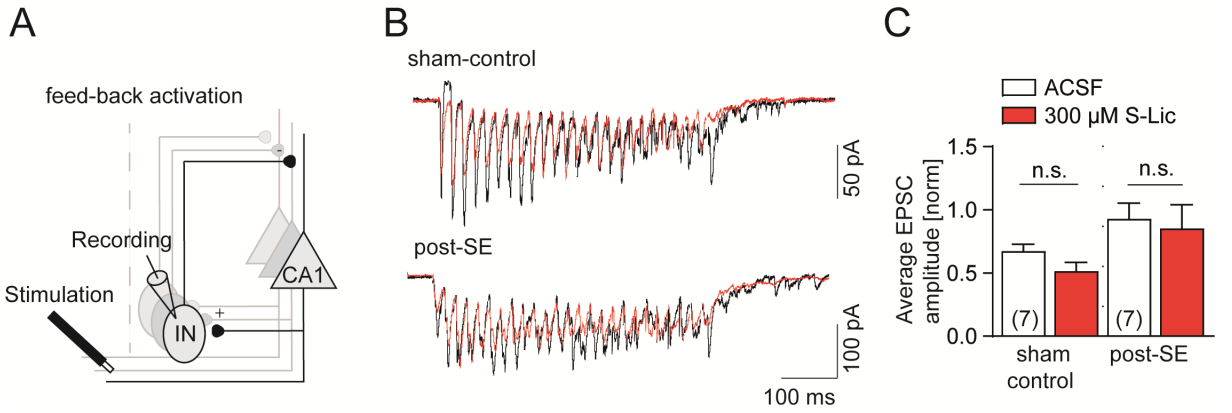

Figure 14: Dissection of S-Lic effects on activation of feed-back interneurons ***A*** Recording configuration to elicit feed-back activation in CA1 feed-back interneurons. ***B*** Representative recordings of feed-back EPSCs with application of 300 µM S-Lic (red traces). ***C*** Quantification of the mean EPSC amplitude of the 50 Hz stimulation train during ACSF and washin of 300 µM S-Lic for sham-control and post-SE animals. Normalized to first EPSC amplitude in 50 Hz train during ACSF. n.s. indicates p>0.05 for RM two-way ANOVA using Bonferroni's multiple comparison test. n numbers indicated in parentheses.

3.8. S-Lic effects on intrinsic firing of feed-back interneurons

Finally, I determined whether S-Lic influences intrinsic properties and firing behavior of stratum oriens interneurons differently in sham-control and epileptic animals (reconstruction in **Figure 15A**). OLMs are driven by strongly facilitating feed-back EPSCs (**Figure 15A**, insets) and show regular firing patterns with maximum firing rates between 30-40 Hz both in sham-control and epileptic animals (**Figure 15B**). S-Lic inhibited repetitive firing both in sham-control and post-SE animals at 300 µM concentrations (representative examples in **Figure 15B**). An analysis of the effects of S-Lic at current injections at which maximal firing rates were observed in the ACSF condition showed that 300 µM S-Lic significantly reduced maximal firing in sham-control and post-SE animals (**Figure 15E,** RM two-way ANOVA using post-hoc Bonferroni's multiple comparison test for ACSF vs. S-Lic, sham-control: reduction of 52.1±8.0 %, $p_{(4.74\ 28)}$=0.0001, post-SE: reduction of 36.6±9.0 %, $p_{(3,641\ 28)}$=0.0022). However, I did not find a significant difference in S-Lic effects on sham-control and post-SE animals, which could explain the AED-evoked plasticity in post-SE animals (comparison of sham-control vs. post-SE using RM two-way ANOVA, F(1, 28)=1.991 p=0.1692).

When analyzing the effects of 300 µM S-Lic on active and passive properties, I found that S-Lic reduces the sag ratio. Additionally, I found that S-Lic increase max. dV/dt and half width of action potentials in stratum oriens interneurons (**Table 3**). However, I did not observe any differences in active and passive properties between sham-control and epileptic animals (**Table 3,** for absolute values see **Table 4** in appendix).

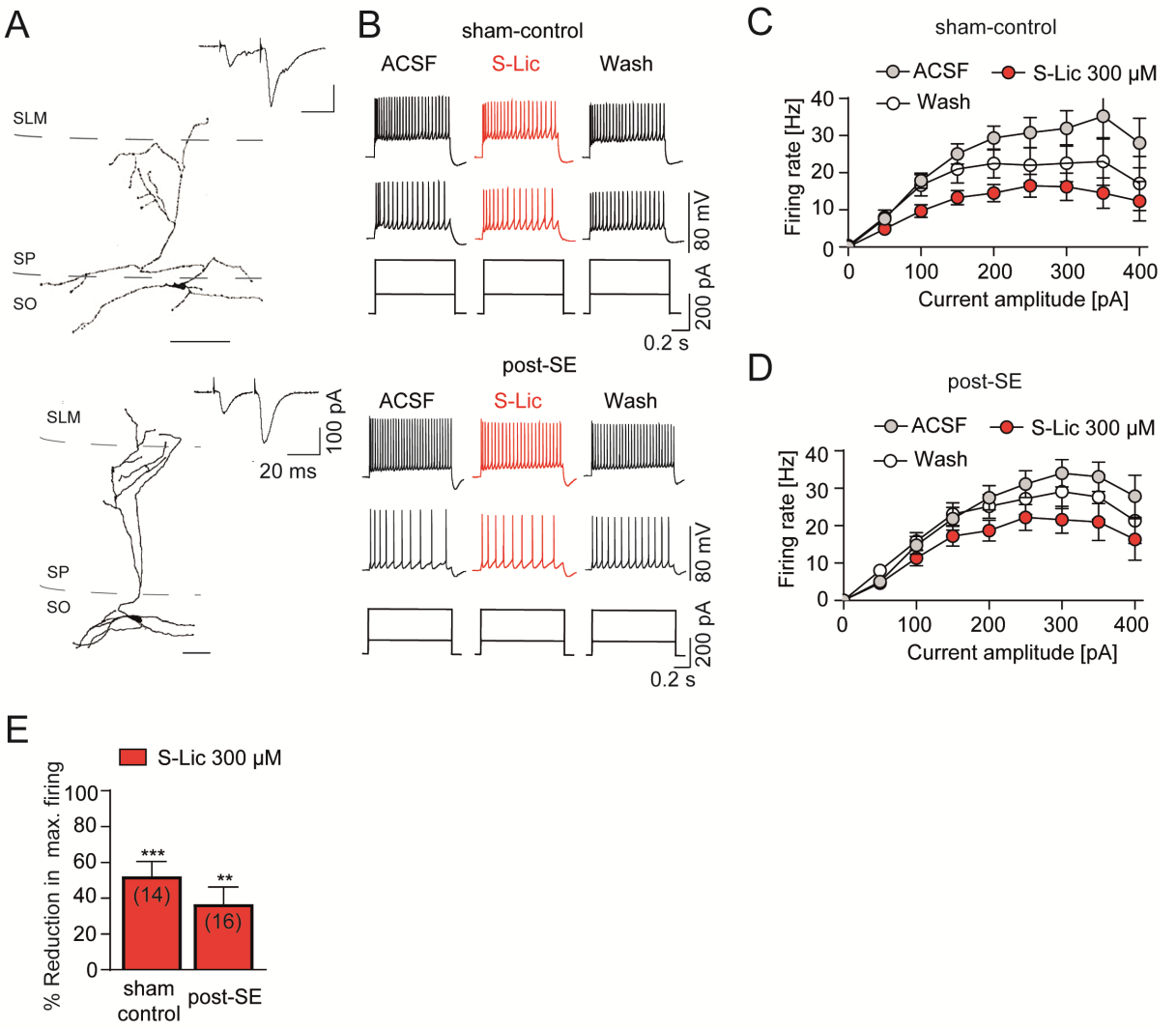

Figure 15: S-Lic effects on firing properties of feed-back interneurons. ***A*** Morphological reconstruction of a representative feed-back interneuron in sham-control and post-SE animals (upper reconstruction and lower reconstruction, respectively). SP, Stratum pyramidale; SO, Stratum oriens. Scale bar 100 µM. Inset with representative recordings of feed-back activation of OLM interneurons with potentiated EPSC amplitudes in sham-control and post-SE animals. ***B*** Effects of 300 µM S-Lic on intrinsic firing induced by current injection (1000 ms) for sham-control (upper panel) and post-SE animals (lower panel). ***C, D*** Corresponding input-output relationship of the average firing rate during 1000 ms current injection versus the current amplitude for sham-control and post-SE animals respectively. ***E*** Percent reduction in the maximal firing rate for 300 µM S-Lic for sham-control and post-SE animals. ** and *** represent $p<0.01$ and 0.001 for RM two-way ANOVA using Bonferroni's multiple comparison test. n numbers indicated in parentheses.

Table 3: Effects of S-Lic on active and passive properties of stratum oriens interneurons. R_m: membrane resistance, tau: membrane time constant, C_m: membrane capacitance, Sag ratio: % reduction of hyperpolarization by h-current during a -100 pA current step, mAHP: medium after hyperpolarization, AHP delay: time of afterhyperpolarization after peak, Threshold: action potential threshold, max. dV/dt: maximal action potential slope, Half width: action potential width at half-maximal amplitude between threshold and peak. Two-way ANOVA, p-values are considered significant after Bonferroni correction with p<0.0055.

	300 µM		
R_m (MOhm)	Interaction	F=0.4099	P=0.4099
	S-Lic	F=6.166	P=0.0195
	Epilepsy	F=4.131	P=0.0521
tau (ms)	Interaction	F=0.247	P=0.6234
	S-Lic	F=0.4765	P=0.4961
	Epilepsy	F=5.13	P=0.0321
C_m (pF)	Interaction	F=0.03928	P=0.8444
	S-Lic	F=0.5358	P=0.4707
	Epilepsy	F=0.001489	P=0.9695
Sag ratio	Interaction	F=2.455	P=0.1288
	S-Lic	F=13.73	P=0.0010*
	Epilepsy	F=0.1872	P=0.6687
mAHP amplitude (mV)	Interaction	F=0.4806	P=0.4941
	S-Lic	F=0.1954	P=0.6620
	Epilepsy	F=0.0002415	P=0.9877
AHP delay (ms)	Interaction	F=0.2087	P=0.6516
	S-Lic	F=13.09	P=0.0013*
	Epilepsy	F=0.5845	P=0.4514
Threshold (mV)	Interaction	F=0.2942	P=0.5920
	S-Lic	F=2.974	P=0.0961
	Epilepsy	F=0.5938	P=0.4476
max. dV/dt (V/s)	Interaction	F=0.7072	P=0.4078
	S-Lic	F=18.33	P=0.0002*
	Epilepsy	F=0.7457	P=0.3954
Half width (ms)	Interaction	F=2.615	P=0.1175
	S-Lic	F=13.21	P=0.0012*
	Epilepsy	F=0.8407	P=0.3673

4. Discussion

In this work, I investigated the effects of the AED S-Lic, which is the active metabolite of ESL. It is a once-daily anticonvulsant used for adjunctive therapy in epilepsy patients with focal onset seizures. It was developed as a structural analog of CBZ. Both of these AEDs have their main effects on VGSCs. Previous studies have mainly investigated sodium blocker effects on excitatory cells. So far little is known about the effects of AEDs on inhibitory cells and inhibitory networks in the brain. In this work, I find that S-Lic reduces firing not only of excitatory CA1 principal cells but also of stratum radiatum and stratum oriens interneurons both in sham-control and epileptic animals. Additionally, S-Lic reduces feed-forward inhibition in both sham-control and epileptic animals, but results in a plastic up-regulation of feed-back inhibition only in epileptic animals.

4.1. S-Lic effects on active and passive properties of principal cells and interneurons

In human epilepsy, a high number of patients suffer from pharmacoresistance to AED therapy. The frequently used AED CBZ to treat patients with chronic refractory temporal lobe epilepsy, has been shown to be less effective in blocking VGSCs in experimental epilepsy (Remy et al., 2003a, 2003b). However, one novel sodium channel acting AED S-Lic, which is structurally related to CBZ, has been shown to potentially overcome cellular resistance mechanism and to maintain use-dependent blocking effects both in human and experimental epilepsy (Doeser et al., 2015). Therefore, in my first experiments I tested the effects of high (300 µM) and low (100 µM) concentrations of S-Lic on the active and passive properties of principal CA1 cells. Indeed, I found that high concentrations (300 µM) of S-Lic were able to reduce not only maximum firing of principal CA1 cells, but also early AP firing in the train for both sham-control and post-SE animals. These results show that S-Lic is still able to reduce firing of excitatory cells in epileptic tissue and to maintain its use-dependent blocking effects.

However, 100 µM S-Lic had only significant effects on the firing of CA1 principal cells in epileptic animals.

Quantification of the S-Lic effects on active and passive properties of CA1 principal cells revealed only small effects of 100 µM S-Lic on AHP delay, sag ratio and AHP threshold. Only effects on sag ratio were consistently changed with high concentrations of S-Lic. However, the effects of 100 µM S-Lic did not translate into reduced firing in both animal groups as mentioned above. However, high and low concentrations of S-Lic affected sag ratio. Sag ratio is considered to be modulated by the activation of HCN channels (Lüthi and McCormick, 1998). So far no study investigating the effects of S-Lic on different ion channels could reveal effects on HCN channels (for review see Soares-da-Silva et al., 2015). I further analyzed the absolute values and found consistent effects of S-Lic on sag ratio but they were very small with changes in the range of 1 to 3 mV. These small effects on sag ratio seem to be irrelevant for the generation of action potentials. However, the reduction of maximum firing rates in excitatory CA1 principal cells by 300 µM S-Lic is in line with previous published data (Bonifácio et al., 2001; Hebeisen et al., 2011; Doeser et al., 2015).

As mentioned above, S-Lic mainly acts on VGSCs. VGSCs are expressed in excitatory cells like PCs but also in inhibitory cells of the brain. Therefore, I tested the effects of S-Lic on two interneuron classes in CA1, which are in involved in important inhibitory microcircuits. Both classes of interneurons (feed-forward interneurons with their soma in stratum radiatum and feed-back interneurons with their soma in stratum oriens) were affected only by high concentrations of S-Lic. 300 µM S-Lic did not only reduce maximum firing of both interneuron types but also had an increased effect with the duration of current injection. For stratum radiatum interneurons, S-Lic had no effects on active or passive properties. The effects on stratum oriens interneurons on e.g. sag ratio or half width were small, comparable to effects of S-Lic observed in CA1 PCs. For both of these interneuron types I did not find any significant differences when comparing active and passive properties of sham-control vs. post-SE animals.

The effect of the AED S-Lic in blocking not only excitatory cells but also inhibitory cells is not easily reconciled, considering the important function of inhibition to counterbalance hyperactivity in the brain. However, the role of interneurons is not only limited to provide synaptic inhibition. Some interneuron types play an important role in synchronizing neuronal networks via e.g. precisely timed inhibition (McBain and

Fisahn, 2001). A seizure is considered to be an event with highly synchronized neuronal activity. Therefore, blocking inhibitory cells by an AED and thereby reducing synchronicity could be one possible mechanism to reduce seizure spread. However, I only tested effects of S-Lic on inhibitory interneurons during intrinsic firing and omitted the effects of S-Lic on firing of these cells during the recruitment in network events. However, most of the AEDs used in clinical practice rather act via a reduction of excitation (for review see Bialer and White, 2010) and an AED mechanism of action via a reduction of inhibition has to be further validated. Finally, S-Lic's inhibitory effects on specific inhibitory neurons in combination with inhibitory effects on excitatory cells may be an effective mechanisms of action as an antiepileptic drug.

Both experiments in excitatory principal cells and inhibitory interneurons in CA1 revealed that S-Lic affects firing behavior mostly in high and not in low concentrations. On account of this, the question arises, how relevant high concentrations of S-Lic are in human clinical practice? In human studies investigating plasma concentrations of S-Lic, concentrations ranged between 9.7 and 23 mg/l, which roughly correspond to 100 µM S-Lic used in this work (Perucca and Tomson, 2011). However, one has to consider the preference for S-Lic to stick to tissue material in a ratio of about 50:1 (Soares-da-Silva et al., 2015). In a mouse study, levels of S-Lic were measured for the total brain mass with a concentration of 22 nmol/g. Considering that S-Lic preferentially sticks to tissue material and in particular to bilipidic membranes, which constitute about 10-12 % of the total brain mass, the study corrected the concentration of S-Lic to ~ 183 µMol/l, which is 8.3 times higher than that measured directly in total brain volume (Pratt et al., 1969; Anon, 1972; Banay-Schwartz et al., 1992). These studies support the use of high concentrations (300 µM) of S-Lic in experimental epilepsy.

4.2. S-Lic effects on specific sodium channels

In contrast to other AEDs like CBZ, S-Lic has been shown to act on specific VGSCs in the brain. A recent study has shown that S-Lic affects slow inactivation dependence of specific sodium channel subtypes. S-Lic shifts the voltage dependence of $Na_v1.2$ and $Na_v1.6$ to more negative potentials, leaving $Na_v1.1$ and $Na_v1.3$ unaffected (Holtkamp et al., 2018). Mostly $Na_v1.2$ and $Na_v1.6$ are considered to be expressed in excitatory cells and $Na_v1.1$ mainly in GABAergic interneurons (Yu et al., 2006; Ogiwara et al., 2007). This is in line with my results of S-Lic reducing firing of excitatory cells in CA1 but cannot explain my observed effects of S-Lic on firing of feed-forward and feed-back

interneurons. However, a more recent study using light and electron microscopy investigated different sodium channel subtype expression in pre- and post-synaptic sites in the rat hippocampus (Johnson et al., 2017). They showed immunoreactivity for $Na_v1.1$, $Na_v1.2$ and $Na_v1.6$ in different layers of the hippocampus. Interestingly, they e.g. showed that dendritic structures in stratum lacunosum moleculare and stratum oriens express $Na_v1.2$ and $Na_v1.6$ and $Na_v1.1$ and $Na_v1.6$, respectively. These layers include among others, dendrites of stratum oriens and stratum radiatum interneurons. Additionally, they showed that axonal structures in stratum lacunosum moleculare and stratum radiatum express $Na_v1.1$, $Na_v1.2$ and $Na_v1.6$ and $Na_v1.1$ and $Na_v1.2$, respectively. These layers contain axons of stratum oriens and stratum radiatum interneurons. These results could explain why S-Lic reduces firing not only of excitatory but also of inhibitory cells. However, more research has to be conducted to confirm expression patterns of different sodium channel subtypes expressed in different cell types.

To investigate effects of S-Lic on different cell types in epileptic animals I used the chemoconvulsant pilocarpine model of mTLE. The pilocarpine model was first described in 1983 and showed that systemic intraperitoneal administration in rodents leads to motor limbic seizures which evolve into SE (Turski et al., 1983). The pilocarpine model represents a well-established animal model to investigate effects of AEDs on experimental tissue for several reasons. Pilocarpine treatment results in widespread damage of the olfactory cortex, amygdala, thalamus, neocortex, hippocampus and substantia nigra (Turski et al., 1989). Hippocampal lesions caused by this model are very similar to hippocampal sclerosis observed in human patients suffering from mTLE (Turski et al., 1984; Tremblay et al., 1985; Cavalheiro et al., 1991). Additionally, a study investigating the anticonvulsant efficacy of the AED levetiracetam (LEV) showed a tolerance development to LEV in a subgroup of animals treated with pilocarpine (Glien et al., 2002). Indeed, other studies investigating the effects of the AED CBZ, showed that in pilocarpine treated animals the use-dependent blocking effect of CBZ is lost, suggesting a development of pharmacoresistance against CBZ, similar to pharmacoresistance observed in human TLE (Remy et al., 2003a; Doeser et al., 2015; Beckonert et al., 2018). Therefore, the pilocarpine model is a useful candidate to investigate effects of novel AEDs in epileptic and even pharmacoresistant experimental tissue. The use of the pilocarpine model enables me to compare my results with previous published data mentioned above.

4.3. Effects of S-Lic on inhibitory systems

I have systematically investigated the effects of S-Lic on inhibitory systems in the CA1 area of the hippocampus. This structure is strongly affected in mTLE, including e.g. hippocampal sclerosis with cell loss in CA1 of excitatory and inhibitory cells (see introduction and Engel, 1996; Blümcke et al., 2013). I have used selective stimulation techniques, which allow me to assess the function of canonical inhibitory motifs (Pouille and Scanziani, 2004a; Pothmann et al., 2014). I show effects of S-Lic on feed-forward inhibition with 300 µM and not with 100 µM. Feed-back inhibition was insensitive to S-Lic even at high concentrations of 300 µM. This leads to the conclusion, that not only firing of different cell types, as discussed in 4.1, but also inhibitory CA1 microcircuits are spared by low concentrations of S-Lic.

In contrast to 100 µM of S-Lic, 300 µM showed strong inhibitory effects on feed-forward inhibition. These effects were substantial with reductions of the initial feed-forward IPSC in sham-control and epileptic animals, respectively. I could exclude that effects of S-Lic on stimulation of CA3 axons or on excitatory drive onto feed-forward interneurons could account for inhibitory effects on feed-forward inhibition. However, I found that intrinsic firing of putative feed-forward interneurons in epileptic animals is reduced by high concentrations of S-Lic. In sham-control animals S-Lic reduces intrinsic firing of putative feed-forward interneurons with 29.4 %, which is statistically not significant, but could be biologically relevant. Therefore, feed-forward inhibition is most likely reduced via reduced firing of interneurons contributing to feed-forward inhibition. However, closer investigation of the reduction of firing in different time windows during the current injection revealed only small effects of S-Lic on the firing of the first AP's in the train. This leads to the question, whether the reduction in firing of feed-forward interneurons can account for the reduced first feed-forward IPSCs. However, one has to keep in mind, that intrinsic firing patterns of cells cannot be equally translated into firing patterns during network recruitment. In line with this, a study investigating the effects of the AED CBZ on the firing of basket cells, involved in feed-forward inhibition, showed that CBZ reduced firing induced by current injection, but left feed-forward inhibition unaffected. A possible explanation would be that the strongly depressing synaptic recruitment of basket cells during feed-forward inhibition does not allow for the development of a use-dependent Na^+ channel block (Pothmann et al., 2014). These results indicate, that due to the nature of synaptic recruitment via Schaffer collaterals, S-Lic and other AEDs like CBZ may be unable to develop a use-

dependent block of interneurons involved in feed-forward inhibition. However, in this study we did not investigate other classes of interneurons which are considered to be involved in feed-forward inhibition in the hippocampus, like different types of basket cells (for review see Thomas Klausberger and Peter Somogyi, 2008). Therefore, we cannot exclude effects of S-Lic on other types of interneurons being responsible for the reduction of feed-forward inhibition.

Another possibility of how S-Lic reduces feed-forward inhibition could be due to effects on the inhibitory synapse of feed-forward interneurons onto CA1 PCs. I did not investigate the effects on this particular synapse, however, one potential candidate which is affected by S-Lic is the T-type calcium channel $Ca_v3.2$. A study by Doeser et. al showed that S-Lic strongly blocks T-type calcium channels $hCa_v3.2$ (human cDNA), which were stably expressed in HEK293 cells. T-type calcium channels belong to the family of low voltage activated Ca^{2+} channels (Perez-Reyes, 1999) and are involved in cell excitability, shape neuronal firing patterns and modulate neurotransmitter release (Perez-Reyes et al., 1998; Cain and Snutch, 2010). But are T-type calcium channels expressed at synapses made by inhibitory feed-forward interneurons onto CA1 PCs? In the hippocampus T-type $Ca_v3.2$ expression has been repeatedly observed in the granule cell layer of the dentate gyrus as well as in PC layers of CA1, CA2 and CA3 (Talley et al., 1999; McKay et al., 2006; Bernal Sierra et al., 2017). CA1 PCs show immunoreactivity for $Ca_v3.2$ ranging from soma over proximal to mid dendrites (McKay et al., 2006). These areas are targeted by feed-forward interneurons and thereby a block of T-type $Ca_v3.2$ currents by S-Lic could potentially reduce feed-forward inhibition in CA1 PCs.

Unlike feed-forward inhibition, feed-back inhibition was not reduced during the washin of 300 µM S-Lic. This contrasted with the reduction of neuronal firing in putative feed-back interneurons like OLM's. In contrast to basket cells (see above), OLMs are synaptically recruited by increasing inputs and result in late-persistent EPSPs (Pouille and Scanziani, 2004b). Therefore, the loss of a use-dependent Na^+ channel block due to reduced synaptic recruitment seems to be unlikely. Interestingly, the same study investigating the recruitment of basket cells also examined the recruitment of OLMs in the feed-back circuit and the effects of the AED CBZ on these. They also find reduced intrinsic firing of OLM cells during the washin of CBZ but no effects during the synaptic recruitment, although OLMs were reliably recruited during feed-back activation

(Pothmann et al., 2014). So far, there is no adequate explanation for this phenomenon. However, as mentioned above, the intrinsic firing of cells cannot be directly translated into their response during network recruitment like feed-back inhibition. To investigate the involvement of OLM firing during network activity, it would be desirable to record firing behavior of OLMs during the recruitment of feed-back inhibition.

To study inhibitory network systems in the hippocampus I used stimulation patterns to induce neuronal activity, which is present during physiologically relevant network activity (Thomas Klausberger and Peter Somogyi, 2008). Gamma- (25-100 Hz) and theta-band (4-8 Hz) oscillations have been shown to occur in the hippocampal formation (Buzsáki, 2005; Colgin and Moser, 2010). Both forms of oscillations have been associated with a number of cognitive functions like feature recognition, sensory information processing, associative learning and memory (Colgin and Moser, 2010; Yamamoto et al., 2014) and have also been related to specific interneurons involved in different inhibitory micronetworks (for reviews see, Whittington and Traub, 2003; Kullmann, 2011). Due to the nature of the feed-forward stimulation, I mainly stimulate interneurons which are targeted by Schaffer collaterals like Schaffer-collateral-associated interneurons in CA1 stratum radiatum or basket cells. Schaffer collateral inputs have been proposed to be the origin of hippocampal gamma oscillations *in vivo* (Csicsvari et al., 2003). For feed-back recruitment, I stimulated in the alveus of CA1 and thereby recruited mainly stratum lacunosum moleculare interneurons (OLM cells), which innervate distal dendrites in the stratum lacunosum moleculare of CA1 PCs. OLM cells receive their majority of inputs directly from local PCs, involving this cell type in particular in feed-back inhibition (Blasco-Ibáñez and Freund, 1995). OLMs operate on a slower timescale and have been shown to be involved in theta oscillations (Gloveli et al., 2005). Therefore, I tested different stimulation frequencies ranging between 1 and 100 Hz to investigate the effects of S-Lic on physiologically relevant oscillations.

However, one has to keep in mind, that due to the nature of the stimulation, I investigate isolated networks. The effects of S-Lic on a complete intact network in the hippocampus cannot be revealed by my data. Additionally, the network connectivity *in vivo* will be much more complex. However, this simplified approach ensures that the observed effects of S-Lic can be assigned to specific synaptic connections.

In this work, I used a bipolar electrode to stimulate network activity in the hippocampus. This approach offers several advantages. First, it offers the opportunity to stimulate in

a frequency range which is physiologically relevant in the hippocampus, ranging from theta to gamma frequencies. Second, to study feed-forward and feed-back inhibition, it is possible to stimulate canonical inhibitory circuits. Its implementation is easy and does not involve long preparation times like e.g. virus expression for the usage of optogenetic tools. To investigate specific neuronal populations and to reveal their contribution in different neuronal networks, optogenetic tools could be used to control activity of different interneuron types (Karpova et al., 2005; Lima and Miesenböck, 2005; Szobota et al., 2007).

4.4. AED-induced plasticity of inhibition

One unexpected finding was that S-Lic persistently increased feed-back inhibition after washout of S-Lic only in epileptic animals. This effect seems to be specific for S-Lic, as other AEDs like CBZ, LTG or PHT did not induce a potentiation. Additionally, I only observed this effect in feed-back and not in feed-forward inhibition. Due to the nature of the alveus stimulation, the main interneurons participating in this feed-back inhibition are stratum oriens interneurons, which target CA1 PCs at their distal dendrites in stratum lacunosum moleculare. A study by Lamsa et al. has shown that these types of interneurons demonstrate a specific form of potentiation, which they termed Anti-Hebbian LTP (Lamsa et al., 2007b). Anti-Hebbian LTP is dependent on influx of Ca^{2+} through CP-AMPAR and activation of T-type Ca^{2+} channels (Nicholson and Kullmann, 2017). AMPA receptors consist in general of a combination of the subunits GluR1, GluR2, GluR3 and GluR4 and are expressed in neurons and glia throughout the brain (Wisden and Seeburg, 1993; Henley and Wilkinson, 2016). The majority of AMPARs consist of a GluR2 subunit that is produced by RNA editing and leaves the channel impermeable to Ca^{2+} (Sommer et al., 1991; Verdoorn et al., 1991). If the AMPAR either lacks GluR2 or shows an unedited GluR2 subunit, it is permeable to Ca^{2+}. CP-AMPA receptor-dependent LTP is prevented by postsynaptic depolarization, as intracellular polyamines block CP-AMPAR at depolarized potentials (Kullmann and Lamsa, 2007; Lamsa et al., 2007b). It was also shown that Anti-Hebbian LTP is not present at Schaffer collateral synapses on interneurons in the stratum radiatum (Lamsa et al., 2007b).

I show that potentiation of feed-back inhibition is prevented by blocking CP-AMPA receptors, suggesting that they indeed play a role in LTP induction by S-Lic. Previous literature has suggested that expression of CP-AMPAR is increased after SE, due to

down-regulation of GluR2 subunits (Friedman et al., 1994; Oguro et al., 1999; Prince et al., 2000; Sommer et al., 2001; Liang and Jones, 2018; Sanchez et al., 2018). Therefore, I recorded CP-AMPAR mediated EPSCs in potential feed-back interneurons but did not find any significant difference between sham-control and epileptic animals. These results suggest that differential expression of GluR2 subunit cannot account for the promotion of anti-Hebbian LTP in epileptic animals. However, my recordings only give an indirect hint of GluR2 expression levels and I cannot exclude that my method was not sensitive enough to measure differences in CP-AMPAR mediated EPSCs between sham-control and epileptic animals. Immunohistochemistry investigating the expression of GluR2 subunits in different cell types are quite advanced techniques but would be desirable to directly detect changes in expression levels between sham-control and epileptic animals.

Another possibility why S-Lic promotes anti-Hebbian LTP could be explained by a reduced block of CP-AMPAR in epileptic tissue. A study by Royeck et al. show that after SE, intracellular polyamines, which are able to block CP-AMPAR, are reduced in hippocampal tissue (Royeck et al., 2015). Therefore, I recorded excitatory currents in potential feed-back interneurons and could observe an increasing amplitude over time due to the washout of spermine and a reduced block of CP-AMPAR. However, I could not observe any differences in changes of EPSC amplitudes between sham-control and epileptic animals. These results reveal no measurable difference in spermine levels in potential feed-back interneurons between sham-control and epileptic animals. This suggests that spermine levels are not involved in the promotion of anti-Hebbian LTP in epileptic tissue. However, my recordings only provide indirect measures of spermine levels. It would be desirable to directly detect levels of spermine in inhibitory interneurons involved in anti-Hebbian LTP using e.g. high pressure liquid chromatography (HPLC).

As stated above, anti-Hebbian LTP can be blocked by depolarization of the postsynapse. Therefore, it would be interesting to investigate, whether S-Lic affects depolarization levels of putative feed-back interneurons. Another hypothesis explaining promoted anti-Hebbian LTP in putative feed-back interneurons would be that S-Lic reduces membrane depolarization of these cells and thereby increases the chance of anti-Hebbian LTP. Perforated patch methods would allow to record membrane potentials and even LTP of cells without disturbing cytoplasmic

homeostasis. Unfortunately, despite significant efforts, I was not able to obtain viable perforated patch recordings from OLM interneurons in epileptic animals. This was due to the very difficult experimental conditions: to patch in epileptic and necrotic tissue from a small number of very specific interneurons. However, I was able to obtain a small number of feed-back EPSP recordings in whole-cell mode of OLM interneurons. Due to the difficult experimental conditions I recorded only a small number of interneurons (n=6 for each group of sham-control and post-SE animals), but I could observe a trend of S-Lic reducing depolarization in OLM interneurons in epileptic tissue (data not shown here). Due to the small n numbers it is not possible to statistically verify these results, yet they give a first hint that non-Hebbian LTP in OLMs could be enhanced by the presence of S-Lic. In line with this, S-Lic potentially limits membrane depolarization during induction of this form of plasticity in epileptic animals.

Irrespective of the underlying mechanism of AED-induced plasticity, my results suggest that not only short-term but also long-term effects of AEDs on ion channel function should be considered when assessing basic mechanisms of AED actions. But which functional consequences do arise from this proposed AED-induced plasticity of feed-back inhibition in epileptic tissue? Several studies have suggested that dendritic inhibition of principal CA1 cells is reduced in experimental models of epilepsy, due to a reduction in release probability at inhibitory synapses targeting apical dendrites of CA1 PCs and a loss of somatostatin-positive OLM interneurons (Cossart et al., 2001; Pothmann et al., 2019). Dendritic inhibition in CA1 is mainly mediated by OLM interneurons, which are involved in feed-back inhibition as mentioned above. Consequently, a reduced dendritic inhibition in CA1 PCs can lead to a reduced seizure threshold. In line with this, S-Lic-induced increase in feed-back inhibition could counterbalance reduced dendritic inhibition in epileptic tissue.

4.5. Predictions for oscillatory events in the hippocampus

So far I have discussed single effects of S-Lic on individual feed-forward and feed-back inhibitory networks in the hippocampus. But how are interneurons involved in different patterns of oscillation and how could S-Lic affect these? Interneurons are thought to be able to modulate the timing of principal cell discharge and are proposed to be involved in the generation and spread of network oscillations (Cobb et al., 1995; Whittington et al., 1995; Miles et al., 1996; Wang and Buzsáki, 1996; Pouille and Scanziani, 2001b; Bartos et al., 2002). Two well studied network oscillations in the

hippocampus are gamma (30 – 80 Hz) and theta (5 – 12 Hz), which have been proposed to be fundamental mechanisms involved in associative learning, feature recognition, or context-sensitive processing of sensory information (Buzsáki, 1996; Miltner et al., 1999; Rodriguez et al., 1999; Fries et al., 2002; Gruber et al., 2002). Experimental and theoretical studies have suggested that networks of GABAergic interneurons are critically involved in gamma oscillations (Van Vreeswijk et al., 1994; Bragin et al., 1995; Whittington et al., 1995; Penttonen et al., 1998; Bartos et al., 2001) Therefore, I mostly studied networks during 50 Hz stimulation frequencies and will discuss the involvement of interneurons during gamma oscillations. So far several studies have suggested that fast-spiking basket cells expressing parvalbumin (FS-PV) are involved in gamma oscillations (Kawaguchi et al., 1987; Bragin et al., 1995; Hájos et al., 2004). FS-PV have fast signaling properties, like fast-spiking action potential phenotype and high intrinsic resonance frequencies (Pike et al., 2000; Jonas et al., 2004). They are characterized by high mutual interconnectivity through fast synaptic inhibition and electrical coupling (Fukuda and Kosaka, 2000; Bartos et al., 2002; Galarreta and Hestrin, 2002; Hefft and Jonas, 2005). FS-PVs are able to synchronize a large group of excitatory neurons and have been shown to be involved in gamma oscillations (Pike et al., 2000; Hefft and Jonas, 2005). As mentioned above, basket cells, including FS-PVs, also contribute to feed-forward inhibition (Buzsàki and Eidelberg, 1981; Alger and Nicoll, 1982; Pouille and Scanziani, 2001b). In my work I found that S-Lic reduces feed-forward inhibition in sham-control and epileptic tissue. How could this effect of S-Lic on feed-forward inhibition translate into modulation of gamma oscillations, especially in networks of epileptic tissue? To answer this question, it is important to discuss potential changes in epileptic networks. Yu et al. showed that, e.g. the GABA reversal potential (E_{GABA}) in dentate basket cells was depolarized after experimental SE, resulting in increased basket cell frequency by over 30 Hz to the 80-250 Hz range, which is associated with epileptic network events (Yu et al., 2013). A follow-up study using a biophysically based model of specific interneurons involved in gamma oscillations found supporting evidence of increased tonic GABA currents by basket cells after seizure induction (Proddutur et al., 2013), which putatively contribute to pathological high frequency firing observed in human and animal epilepsy (Bragin et al., 1999; Worrell et al., 2004, 2008). In line with this, a reduction of feed-forward inhibition by S-Lic, as shown in my data, could putatively restrict pathological focal high frequency firing of basket cells in epileptic tissue.

In summary, a reduced feed-forward inhibition by S-Lic resulting in reduced pathological focal high frequency firing of specific interneurons and the AED-induced plasticity in feed-back inhibition to scale up dendritic inhibition of CA1 PCs to increase seizure threshold could support the use of S-Lic as an effective AED in the treatment of partial onset seizures.

5. Appendix

5.1. Abbreviations

ACSF: artificial cerebrospinal fluid

AED: antiepileptic drug

AMPA: α-amino-3-hydroxy-5-methyl-4-isoxazolepropionic acid

AP: action potential

BC: basket cell

CBZ: carbamazepine

CCK: cholecystokinin

CNS: central nervous system

CP-AMPAR: Ca^{2+} permeable AMPA receptors

DG: dentate gyrus

EC: entorhinal cortex

EEG: electroencephalography

EGTA: ethylene glycol tetraacetic acid

EPSC: excitatory postsynaptic current

EPSP: excitatory postsynaptic potential

ESL: Eslicarbazepine acetate

fAHP: fast after hyperpolarizing potential

FB: feed-back

FS-PC: fast spiking basket cells expressing parvalbumin

GABA: g-amminobutyric acid

GluR: glutamate receptor

HEPES: 4-(2-hydroxyethyl)-1-piperazineethanesulfonic acid

HPLC: high pressure liquid chromatography

HS: Hippocampal sclerosis

ILAE: International League Against Epilepsy

I_{NaP}: Persistent sodium current

I_{NaT}: Transient sodium current

IPSC: inhibitory postsynaptic current

LTG: lamotrigine

MRI: magnetic resonance imaging

mTLE: mesial temporal lobe epilepsy

NMDA: N-Methyl-d-aspartate

OLM: oriens-lacunosum moleculare

PC: pyramidal cell

PHT: phenytoin

PSC: postsynaptic current

PSP: postsynaptic potential

PV: parvalbumin

R_{in}: input resistance

S-Lic: eslicarbazepine

SE: status epilepticus

SEM: standard error of the mean

SLM: stratum lacunosum moleculare

SO: stratum oriens

SP: stratum pyramidale

SR: stratum radiatum

SUB: subiculum

SST: somatostatin

Stim: Stimulus

TLE: temporal lobe epilepsy

VGSC: voltage-gated sodium channel

5.2. Supplement table

Table 4: Active and passive properties in CA1 PCs and CA1 interneurons in sham-control and epileptic rats. Rm: membrane resistance, tau: membrane time constant, Cm: membrane capacitance, Sag ratio: % reduction of hyperpolarization by h-current during a -100 pA current step, mAHP: medium after hyperpolarization, AHP delay: time of afterhyperpolarization after peak, Threshold: action potential threshold, max. dV/dt: maximal action potential slope, Half width: action potential width at half-maximal amplitude between threshold and peak.

	Sham-control	**Post SE**
Pyramidal cells	n=17	n=17
R_m (MOhm)	223.47 ± 17.53	159.03 ± 19.48
tau (ms)	18.06 ± 2.31	12.74 ± 1.23
C_m (pF)	86.06 ± 10.21	90.21 ± 9.21
Sag ratio	0.94 ± 0.00	0.95 ± 0.09
mAHP amplitude (mV)	-6.25 ± 0.66	-8.70 ± 1.10
AHP delay (ms)	9.58 ± 2.41	12.60 ± 2.26
Threshold (mV)	-56.68 ± 0.75	-55.60 ± 5.45
max. dV/dt (V/s)	202.40 ± 13.66	236.66 ± 25.99
Half width (ms)	1.60 ± 0.06	1.41 ± 0.11
Stratum radiatum IN	n=14	n=16
R_m (MOhm)	370.73 ± 39.85	355.41 ± 28.57
tau (ms)	11.78 ± 1.10	14.01 ± 1.04
C_m (pF)	33.43 ± 2.72	41.43 ± 2.74
Sag ratio	0.92 ± 0.01	0.91 ± 0.01
mAHP amplitude (mV)	-11.22 ± 0.96	-9.26 ± 0.89
AHP delay (ms)	4.09 ± 0.36	4.35 ± 0.57
Threshold (mV)	-55.39 ± 1.00	-53.90 ± 1.26
max. dV/dt (V/s)	147.29 ± 16.97	138.19 ± 16.68
Half width (ms)	1.23 ± 0.08	1.24 ± 0.11
Stratum oriens IN	n=14	n=16
R_m (MOhm)	354.73 ± 21.46	277.65 ± 30.87
tau (ms)	11.99 ± 0.98	9.00 ± 1.24
C_m (pF)	33.28 ± 2.87	33.49 ± 2.87
Sag ratio	0.88 ± 0.01	0.88 ± 0.01
mAHP amplitude (mV)	-17.71 ± 1.55	-17.28 ± 1.39
AHP delay (ms)	3.44 ± 0.38	4.06 ± 0.64
Threshold (mV)	-54.41 ± 1.96	-56.60 ± 1.35
max. dV/dt (V/s)	139.12 ± 15.97	145.02 ± 9.33
Half width (ms)	1.00 ± 0.06	0.97 ± 0.05

6. Literature

Akaike N, Inomata N, Yakushiji T (1989) Differential effects of extra- and intracellular anions on GABA-activated currents in bullfrog sensory neurons. J Neurophysiol 62:1388–1399 Available at: http://www.ncbi.nlm.nih.gov/entrez/query.fcgi?cmd=Retrieve&db=PubMed&dopt=Citation&list_uids=2557392.

Alger BE, Nicoll RA (1982) Feed-forward dendritic inhibition in rat hippocampal pyramidal cells studied in vitro. J Physiol.

Almeida L, Potgieter JH, Maia J, Potgieter MA, Mota F, Soares-Da-Silva P (2008) Pharmacokinetics of eslicarbazepine acetate in patients with moderate hepatic impairment. Eur J Clin Pharmacol 64:267–273.

Almeida L, Soares-da-Silva P (2007) Eslicarbazepine Acetate (BIA 2-093). Neurotherapeutics 4:88–96.

Ang CW, Carlson GC, Coulter DA (2006) Massive and specific dysregulation of direct cortical input to the hippocampus in temporal lobe epilepsy. J Neurosci.

Anon (1972) Biochemistry and the Central Nervous System 4th edn. By H. McIlwain and H. S. Bachelard. (Pp. 616; illustrated; £7·50.) Churchill Livingstone: Edinburgh. 1971. Psychol Med.

Aronica E, Yankaya B, Troost D, Van Vliet EA, Lopes Da Silva FH, Gorter JA (2001) Induction of neonatal-sodium channel II and III (α-isoform mRNAs in neurons and microglia after status epilepticus in the rat hippocampus. Eur J Neurosci 13:1261–1266.

Ascoli GA et al. (2008) Petilla terminology: Nomenclature of features of GABAergic interneurons of the cerebral cortex. Nat Rev Neurosci.

Banay-Schwartz M, Kenessey A, DeGuzman T, Lajtha A, Palkovits M (1992) Protein content of various regions of rat brain and adult and aging human brain. Age (Omaha).

Barbarosie M, Louvel J, Kurcewicz I, Avoli M, Neurophysiol D JM, Benini R, Biagini G, Barbarosie M, Tancredi V, Avoli M, Dzhala VI, Staley KJ, Neurosci W Ang JC, Carlson GC, Coulter DA, Ene Kurcewicz I (2000) Temporal Lobe Epilepsy. Massive and Specific Dysregulation of Direct Cortical Input to the Hippocampus in CA3-Released Entorhinal Seizures Disclose Dentate Gyrus Epileptogenicity and Unmask a Temporoammonic Pathway. J Neurophysiol.

Bartolomei F, Gastaldi M, Massacrier A, Planells R, Nicolas S, Cau P (1997) Changes in the mRNAs encoding subtypes I, II and III sodium channel alpha subunits following kainate-induced seizures in rat brain. J Neurocytol 26:667–678.

Bartos M, Vida I, Frotscher M, Geiger JRP, Jonas P (2001) Rapid signaling at inhibitory synapses in a dentate gyrus interneuron network. J Neurosci.

Bartos M, Vida I, Frotscher M, Meyer A, Monyer H, Geiger JRP, Jonas P, Heidelberg (2002) Fast synaptic inhibition promotes synchronized gamma oscillations in hippocampal interneuron networks. Proc Natl Acad Sci U S A.

Beckonert N, Opitz T, Pitsch J, Soares da Silva P, Beck H (2018) Polyamine modulation of anticonvulsant drug response: A potential mechanism contributing to pharmacoresistance in chronic epilepsy. J Neurosci:0640–18 Available at: http://www.jneurosci.org/lookup/doi/10.1523/JNEUROSCI.0640-18.2018.

Benini R, Avoli M (2005) Rat subicular networks gate hippocampal output activity in an in vitro model of limbic seizures. J Physiol.

Bernal Sierra YA, Haseleu J, Kozlenkov A, Bégay V, Lewin GR (2017) Genetic tracing of Cav 3.2 t-type calcium channel expression in the peripheral nervous system. Front Mol Neurosci.

Bi G, Poo M (2001) Synaptic Modification by Correlated Activity: Hebb's Postulate Revisited. Annu Rev Neurosci.

Bialer M, White HS (2010) Key factors in the discovery and development of new antiepileptic drugs. Nat Rev Drug Discov 9:68–82 Available at:

https://www.ncbi.nlm.nih.gov/pubmed/20043029.

Blasco-Ibáñez JM, Freund TF (1995) Synaptic Input of Horizontal Interneurons in Stratum Oriens of the Hippocampal CA1 Subfield: Structural Basis of Feed-back Activation. Eur J Neurosci.

Blümcke I et al. (2013) International consensus classification of hippocampal sclerosis in temporal lobe epilepsy: A Task Force report from the ILAE Commission on Diagnostic Methods. Epilepsia 54:1315–1329.

Blümcke I, Coras R, Miyata H, Özkara C (2012) Defining clinico-neuropathological subtypes of mesial temporal lobe epilepsy with hippocampal sclerosis. In: Brain Pathology.

Blümcke I, Pauli E, Clusmann H, Schramm J, Becker A, Elger C, Merschhemke M, Meencke HJ, Lehmann T, Von Deimling A, Scheiwe C, Zentner J, Volk B, Romstöck J, Stefan H, Hildebrandt M (2007) A new clinico-pathological classification system for mesial temporal sclerosis. Acta Neuropathol.

Bonifácio MJ, Sheridan RD, Parada A, Cunha RA, Patmore L, Soares-Da-Silva P (2001) Interaction of the novel anticonvulsant, BIA 2-093, with voltage-gated sodium channels: Comparison with carbamazepine. Epilepsia 42:600–608.

Bormann J, Hamill OP, Sakmann B (1987) Mechanism of anion permeation through channels gated by glycine and gamma-aminobutyric acid in mouse cultured spinal neurones. J Physiol 385:243–286.

Bowie D, Mayer ML (1995) Inward rectification of both AMPA and kainate subtype glutamate receptors generated by polyamine-mediated ion channel block. Neuron.

Brackenbury WJ, Isom LL (2011) Na+ channel β subunits: Overachievers of the ion channel family. Front Pharmacol.

Bragin A, Engel J, Wilson CL, Fried I, Mathern GW (1999) Hippocampal and entorhinal cortex high-frequency oscillations (100-500 Hz) in human epileptic brain and in kainic acid-treated rats with chronic seizures. Epilepsia.

Bragin A, Jando G, Nadasdy Z, Hetke J, Wise K, Buzsaki G (1995) Gamma (40-100 Hz) oscillation in the hippocampus of the behaving rat. J Neurosci.

Bratz (1899) Ammonshornbefunde bei Epileptischen. Arch Psychiatr Nervenkr.

Buckmaster PS, Jongen-Rêlo a L (1999) Highly specific neuron loss preserves lateral inhibitory circuits in the dentate gyrus of kainate-induced epileptic rats. J Neurosci.

Buhl EH, Halasy K, Somogyi P (1994) Diverse sources of hippocampal unitary inhibitory postsynaptic potentials and the number of synaptic release sites. Nature.

Buzsáki G (1996) The hippocampo-neocortical dialogue. Cereb Cortex.

Buzsáki G (2005) Theta rhythm of navigation: Link between path integration and landmark navigation, episodic and semantic memory. Hippocampus.

Buzsàki G, Eidelberg E (1981) Commissural projection to the dentate gyrus of the rat: evidence for feed-forward inhibition. Brain Res.

Cain SM, Snutch TP (2010) Contributions of T-type calcium channel isoforms to neuronal firing. Channels.

Catterall WA (2000) From ionic currents to molecular mechanisms: The structure and function of voltage-gated sodium channels. Neuron.

Catterall WA (2014) Structure and function of voltage-gated sodium channels at atomic resolution. Exp Physiol 99:35–51 Available at: https://www.ncbi.nlm.nih.gov/pubmed/24097157.

Cavalheiro E.A. (1995) The pilocarpine model of epilepsy. Ital J Neurol Sci:33–37.

Cavalheiro EA, Leite JP, Bortolotto ZA, Turski WA, Ikonomidou C, Turski L (1991) Long-Term Effects of Pilocarpine in Rats: Structural Damage of the Brain Triggers Kindling and Spontaneous I Recurrent Seizures. Epilepsia 32:778–782.

Chen S, Su H, Yue C, Remy S, Royeck M, Sochivko D, Opitz T, Beck H, Yaari Y (2010) An Increase in Persistent Sodium Current Contributes to Intrinsic Neuronal Bursting After Status Epilepticus. J Neurophysiol.

Chrobak JJ, Buzsáki G (1995) Temporal structure in spatially organized neuronal ensembles: a role for interneuronal networks. Curr Opin Neurobiol.

Cobb SR, Buhl EH, Halasy K, Paulsen O, Somogyi P (1995) Synchronization of neuronal activity in hippocampus by individual GABAergic interneurons. Nature.

Colgin LL, Moser EI (2010) Gamma Oscillations in the Hippocampus. Physiology.

Cossart R, Dinocourt C, Hirsch JC, Merchan-Perez A, De Felipe J, Ben-Ari Y, Esclapez M, Bernard C (2001) Dendritic but not somatic GABAergic inhibition is decreased in experimental epilepsy. Nat Neurosci.

Cossart R, Esclapez M, Hirsch JC, Bernard C, Ben-Ari Y (1998) GluR5 kainate receptor activation in interneurons increases tonic inhibition of pyramidal cells. Nat Neurosci.

Csicsvari J, Jamieson B, Wise KD, Buzsáki G (2003) Mechanisms of gamma oscillations in the hippocampus of the behaving rat. Neuron.

Davies KG, Hermann BP, Dohan FC, Foley KT, Bush AJ, Wyler AR (1996) Relationship of hippocampal sclerosis to duration and age of onset of epilepsy, and childhood febrile seizures in temporal lobectomy patients. Epilepsy Res.

de Lanerolle NC, Kim JH, Robbins RJ, Spencer DD (1989) Hippocampal interneuron loss and plasticity in human temporal lobe epilepsy. Brain Res.

DeFelipe J (1999) Chandelier cells and epilepsy. Brain.

Dinocourt C, Petanjek Z, Freund TF, Ben-Ari Y, Esclapez M (2003) Loss of interneurons innervating pyramidal cell dendrites and axon initial segments in the CA1 region of the hippocampus following pilocarpine-induced seizures. J Comp Neurol.

Doeser A, Dickhof G, Reitze M, Uebachs M, Schaub C, Pires NM, Bonifácio MJ, Soares-da-Silva P, Beck H (2015) Targeting pharmacoresistant epilepsy and epileptogenesis with a dual-purpose antiepileptic drug. Brain 138:371–387 Available at: https://www.ncbi.nlm.nih.gov/pubmed/25472797.

Doeser A, Soares-da-Silva P, Beck H, Uebachs M (2014) The effects of eslicarbazepine on persistent Na+ current and the role of the Na+ channel β subunits. Epilepsy Res.

Donevan SD, Rogawski MA (1995) Intracellular polyamines mediate inward rectification of Ca(2+)-permeable alpha-amino-3-hydroxy-5-methyl-4-isoxazolepropionic acid receptors. PNAS.

Ellerkmann RK, Remy S, Chen J, Sochivko D, Elger CE, Urban BW, Becker A, Beck H (2003) Molecular and functional changes in voltage-dependent Na+channels following pilocarpine-induced status epilepticus in rat dentate granule cells. Neuroscience 119:323–333.

Engel J (1996) Introduction to temporal lobe epilepsy. In: Epilepsy Research, pp 141–150.

Engel J (2001) Mesial temporal lobe epilepsy: What have we learned? Neuroscientist.

Fisher RS, Acevedo C, Arzimanoglou A, Bogacz A, Cross JH, Elger CE, Engel J, Forsgren L, French JA, Glynn M, Hesdorffer DC, Lee BI, Mathern GW, Moshé SL, Perucca E, Scheffer IE, Tomson T, Watanabe M, Wiebe S (2014) ILAE Official Report: A practical clinical definition of epilepsy. Epilepsia.

Fisher RS, Cross JH, D'Souza C, French JA, Haut SR, Higurashi N, Hirsch E, Jansen FE, Lagae L, Moshé SL, Peltola J, Roulet Perez E, Scheffer IE, Schulze-Bonhage A, Somerville E, Sperling M, Yacubian EM, Zuberi SM (2018a) Instruction manual for the ILAE 2017 operational classification of seizure types. Zeitschrift fur Epileptol.

Fisher RS, Cross JH, French JA, Higurashi N, Hirsch E, Jansen FE, Lagae L, Moshé SL, Peltola J, Roulet Perez E, Scheffer IE, Zuberi SM (2018b) Operational classification of seizure types by the International League Against Epilepsy: position paper of the ILAE Commission for Classification and Terminology. Zeitschrift fur Epileptol.

Fisher RS, Van Emde Boas W, Blume W, Elger C, Genton P, Lee P, Engel J (2005) Epileptic seizures and epilepsy: Definitions proposed by the International League Against Epilepsy (ILAE) and the International Bureau for Epilepsy (IBE). Epilepsia.

Freund TF, Buzsáki G (1996) Interneurons of the hippocampus. Hippocampus.

Freund TF, Katona I (2007) Perisomatic Inhibition. Neuron.

Friedman L, Pellegrini-Giampietro D, Sperber E, Bennett M, Moshe S, Zukin R (1994) Kainate-induced status epilepticus alters glutamate and GABAA receptor gene expression in adult rat hippocampus: an in situ hybridization study. J Neurosci.

Fries P, Schröder JH, Roelfsema PR, Singer W, Engel AK (2002) Oscillatory Neuronal

Synchronization in Primary Visual Cortex as a Correlate of Stimulus Selection. J Neurosci.

Fukuda T, Kosaka T (2000) Gap junctions linking the dendritic network of GABAergic interneurons in the hippocampus. J Neurosci.

Galarreta M, Hestrin S (2002) Electrical and chemical synapses among parvalbumin fast-spiking GABAergic interneurons in adult mouse neocortex. Proc Natl Acad Sci U S A.

Gallagher JP, Higashi H, Nishi S (1978) Characterization and ionic basis of GABA???induced depolarizations recorded in vitro from cat primary afferent neurones. J Physiol 275:263–282.

Gee NS, Brown JP, Dissanayake VUK, Offord J, Thurlow R, Woodruff GN (1996) The novel anticonvulsant drug, gabapentin (neurontin), binds to the α2δ subunit of a calcium channel. J Biol Chem 271:5768–5776.

Gerlach AC, Krajewski JL (2010) Antiepileptic Drug Discovery and Development: What Have We Learned and Where Are We Going? Pharm 3:2884–2899 Available at: https://www.ncbi.nlm.nih.gov/pubmed/27713381.

Glien M, Brandt C, Potschka H, Löscher W (2002) Effects of the novel antiepileptic drug levetiracetam on spontaneous recurrent seizures in the rat pilocarpine model of temporal lobe epilepsy. Epilepsia.

Gloveli T, Dugladze T, Saha S, Monyer H, Heinemann U, Traub RD, Whittington MA, Buhl EH (2005) Differential involvement of oriens/pyramidale interneurones in hippocampal network oscillations in vitro. J Physiol.

Goldin AL (2003) Mechanisms of sodium channel inactivation. Curr Opin Neurobiol.

Grooms SY, Opitz T, Bennett MVL, Zukin RS (2000) Status epilepticus decreases glutamate receptor 2 mRNA and protein expression in hippocampal pyramidal cells before neuronal death. Proc Natl Acad Sci U S A.

Gruber T, Muller MM, Kiel A (2002) Modulation of induced gamma band responses in a perceptual learning task in the human EEG. J Cogn Neurosci.

Hájos N, Mody I (1997) Synaptic communication among hippocampal interneurons:

Properties of spontaneous IPSCs in morphologically identified cells. J Neurosci.

Hájos N, Pálhalini J, Mann EO, Nèmeth B, Paulsen O, Freund TF (2004) Spike timing of distinct types of GABAergic interneuron during hippocampal gamma oscillations in vitro. J Neurosci.

Halasy K, Buhl EH, Lörinczi Z, Tamás G, Somogyi P (1996) Synaptic target selectivity and input of GABAergic basket and bistratified interneurons in the CA1 area of the rat hippocampus. Hippocampus.

Han Z -S, Buhl EH, Lörinczi Z, Somogyi P (1993) A High Degree of Spatial Selectivity in the Axonal and Dendritic Domains of Physiologically Identified Local-circuit Neurons in the Dentate Gyms of the Rat Hippocampus. Eur J Neurosci.

Hebb DO (1949) The Organization of Behavior, Introduction and Chapter 4, " " The first stage of perception : growth of the assembly, pp . xi - xix ,. New York John Wiley Sons.

Hebeisen S, Brady K, Konrad D, Soares-da-Silva P (2011) Inhibitory effects of eslicarbazepine acetate and its metabolites against neuronal voltage-gated sodium channels. Epilepsia 52:257–258.

Hefft S, Jonas P (2005) Asynchronous GABA release generates long-lasting inhibition at a hippocampal interneuron-principal neuron synapse. Nat Neurosci.

Henley JM, Wilkinson KA (2016) Synaptic AMPA receptor composition in development, plasticity and disease. Nat Rev Neurosci.

Holtkamp D, Opitz T, Hebeisen S, Soares-da-Silva P, Beck H (2018) Effects of eslicarbazepine on slow inactivation processes of sodium channels in dentate gyrus granule cells. Epilepsia 59:1492–1506.

Isom LL, Ragsdale DS, De Jongh KS, Westenbroek RE, Reber BFX, Scheuer T, Catterall WA (1995) Structure and function of the β2 subunit of brain sodium channels, a transmembrane glycoprotein with a CAM motif. Cell.

Johnson KW, Herold KF, Milner TA, Hemmings HC, Platholi J (2017) Sodium channel subtypes are differentially localized to pre- and post-synaptic sites in rat hippocampus. J Comp Neurol.

Jonas P, Bischofberger J, Fricker D, Miles R (2004) Interneuron Diversity series: Fast in, fast out--temporal and spatial signal processing in hippocampal interneurons. Trends Neurosci 27:30–40 Available at: https://www.ncbi.nlm.nih.gov/pubmed/14698608.

Jope RS, Morrisett RA, Snead OC (1986) Characterization of lithium potentiation of pilocarpine-induced status epilepticus in rats. Exp Neurol.

Kamboj SK, Swanson GT, Cull-Candy SG (1995) Intracellular spermine confers rectification on rat calcium-permeable AMPA and kainate receptors. J P hysiol.

Karpova AY, Tervo DGR, Gray NW, Svoboda K (2005) Rapid and reversible chemical inactivation of synaptic transmission in genetically targeted neurons. Neuron.

Kawaguchi Y, Katsumaru H, Kosaka T, Heizmann CW, Hama K (1987) Fast spiking cells in rat hippocampus (CA1 region) contain the calcium-binding protein parvalbumin. Brain Res.

Klausberger T (2009) GABAergic interneurons targeting dendrites of pyramidal cells in the CA1 area of the hippocampus. Eur J Neurosci 30:947–957 Available at: https://www.ncbi.nlm.nih.gov/pubmed/19735288.

Klausberger T, Marton LF, O'Neill J, Huck JHJ, Dalezios Y, Fuentealba P, Suen WY, Papp E, Kaneko T, Watanabe M, Csicsvari J, Somogyi P (2005) Complementary roles of cholecystokinin- and parvalbumin-expressing GABAergic neurons in hippocampal network oscillations. J Neurosci.

Kobayashi M, Buckmaster PS (2003) Reduced inhibition of dentate granule cells in a model of temporal lobe epilepsy. J Neurosci.

Koh DS, Burnashev N, Jonas P (1995) Block of native Ca(2+)-permeable AMPA receptors in rat brain by intracellular polyamines generates double rectification. J Physiol.

Kullmann DM (2011) Interneuron networks in the hippocampus. Curr Opin Neurobiol 21:709–716 Available at: https://www.ncbi.nlm.nih.gov/pubmed/21636266.

Kullmann DM, Lamsa KP (2007) Long-term synaptic plasticity in hippocampal interneurons. Nat Rev Neurosci 8:687–699 Available at: http://dx.doi.org/10.1038/nrn2207%5Cnpapers2://publication/doi/10.1038/nrn220

7.

Kwan P, Brodie MJ (2005) Potential role of drug transporters in the pathogenesis of medically intractable epilepsy. Epilepsia.

Lamsa KP, Heeroma JH, Somogyi P, Rusakov DA, Kullmann DM (2007a) Anti-Hebbian Long-Term Potentiation in the Hippocampal Feedback Inhibitory Circuit. Science (80-) 315:1262–1266 Available at: http://www.sciencemag.org/cgi/doi/10.1126/science.1137450.

Lamsa KP, Heeroma JH, Somogyi P, Rusakov DA, Kullmann DM (2007b) Anti-hebbian long-term potentiation in the hippocampal feedback inhibitory circuit. Science (80-).

Liang F, Jones EG (2018) Differential and Time-Dependent Changes in Gene Expression for Type II Calcium/Calmodulin-Dependent Protein Kinase, 67 kDa Glutamic Acid Decarboxylase, and Glutamate Receptor Subunits in Tetanus Toxin-Induced Focal Epilepsy. J Neurosci.

Lima SQ, Miesenböck G (2005) Remote control of behavior through genetically targeted photostimulation of neurons. Cell.

Losonczy A, Zemelman B V, Vaziri A, Magee JC (2010) Network mechanisms of theta related neuronal activity in hippocampal CA1 pyramidal neurons. Nat Neurosci 13:967–972 Available at: https://www.ncbi.nlm.nih.gov/pubmed/20639875.

Lüthi A, McCormick DA (1998) H-current: Properties of a neuronal and network pacemaker. Neuron.

Maccaferri G, Lacaille JC (2003) Interneuron Diversity series: Hippocampal interneuron classifications--making things as simple as possible, not simpler. Trends Neurosci 26:564–571 Available at: https://www.ncbi.nlm.nih.gov/pubmed/14522150.

Macdonald RL, Kelly KM (1995) Antiepileptic Drug Mechanisms of Action. Epilepsia 36:S2–S12.

Magistretti J, Alonso A (1999) Biophysical Properties and Slow Voltage-Dependent Inactivation of a Sustained Sodium Current in Entorhinal Cortex Layer-II Principal Neurons. J Gen Physiol.

Maia J, Almeida L, Falcão A, Soares E, Mota F, Potgieter MA, Potgieter JH, Soares-da-Silva P (2008) Effect of renal impairment on the pharmacokinetics of eslicarbazepine acetate. Int J Clin Pharmacol Ther 46:119–130 Available at: http://www.dustri.com/article_response_page.html?artId=1680&doi=10.5414/CPP46119&L=0.

Marais E, Klugbauer N, Hofmann F (2001) Calcium channel α2δ subunits-structure and Gabapentin binding. Mol Pharmacol 59:1243–1248.

Margerison JH, Corsellis JAN (1966) Epilepsy and the temporal lobes: A clinical, electroencephalographic and neuropathological study of the brain in epilepsy, with particular reference to the temporal lobes. Brain.

McBain CJ, Fisahn A (2001) Interneurons unbound. Nat Rev Neurosci 2:11–23 Available at: http://www.nature.com/doifinder/10.1038/35049047.

McKay BE, McRory JE, Molineux ML, Hamid J, Snutch TP, Zamponi GW, Turner RW (2006) CaV3 T-type calcium channel isoforms differentially distribute to somatic and dendritic compartments in rat central neurons. Eur J Neurosci.

MD IB, MRCPath MT, Wiestler OD (2006) Ammon's Horn Sclerosis: A Maldevelopmental Disorder Associated with Temporal Lobe Epilepsy. Brain Pathol.

Meadows LS, Malhotra J, Loukas A, Thyagarajan V, Kazen-Gillespie KA, Koopman MC, Kriegler S, Isom LL, Ragsdale DS (2002) Functional and biochemical analysis of a sodium channel beta1 subunit mutation responsible for generalized epilepsy with febrile seizures plus type 1. J Neurosci.

Mello LEAM, Cavalheiro EA, Tan AM, Kupfer WR, Pretorius JK, Babb TL, Finch DM (1993) Circuit Mechanisms of Seizures in the Pilocarpine Model of Chronic Epilepsy: Cell Loss and Mossy Fiber Sprouting. Epilepsia.

Miles R, Tóth K, Gulyás AI, Hájos N, Freund TF (1996) Differences between somatic and dendritic inhibition in the hippocampus. Neuron.

Miltner WHR, Braun C, Arnold M, Witte H, Taub E (1999) Coherence of gamma-band EEG activity as a basis for associative learning. Nature.

Nicholson E, Kullmann DM (2017) T-type calcium channels contribute to NMDA

receptor independent synaptic plasticity in hippocampal regular-spiking oriens-alveus interneurons. J Physiol 595:3449–3458 Available at: https://www.ncbi.nlm.nih.gov/pubmed/28134447.

Ogiwara I, Miyamoto H, Morita N, Atapour N, Mazaki E, Inoue I, Takeuchi T, Itohara S, Yanagawa Y, Obata K, Furuichi T, Hensch TK, Yamakawa K (2007) Nav1.1 Localizes to Axons of Parvalbumin-Positive Inhibitory Interneurons: A Circuit Basis for Epileptic Seizures in Mice Carrying an Scn1a Gene Mutation. J Neurosci 27:5903–5914 Available at: http://www.jneurosci.org/cgi/doi/10.1523/JNEUROSCI.5270-06.2007.

Oguro K, Oguro N, Kojima T, Grooms SY, Calderone A, Zheng X, Bennett M V, Zukin RS (1999) Knockdown of AMPA receptor GluR2 expression causes delayed neurodegeneration and increases damage by sublethal ischemia in hippocampal CA1 and CA3 neurons. J Neurosci.

Oliva M, Berkovic SF, Petrou S (2012) Sodium channels and the neurobiology of epilepsy. Epilepsia.

Orman R, Von Gizycki H, Lytton WW, Stewart M (2008) Local axon collaterals of area CA1 support spread of epileptiform discharges within CA1, but propagation is unidirectional. Hippocampus.

Penttonen M, Kamondi A, Acsády L, Buzsáki G (1998) Gamma frequency oscillation in the hippocampus of the rat: Intracellular analysis in vivo. Eur J Neurosci.

Per A, Richard M, David A, Tim B, John OK (2009) The Hippocampal Formation. In: The Hippocampus Book.

Perez-Reyes E (1999) Three for T: Molecular analysis of the low voltage-activated calcium channel family. Cell Mol Life Sci.

Perez-Reyes E, Cribbs LL, Daud A, Lacerda AE, Barclays J, Williamson MP, Fox M, Rees M, Lee JH (1998) Molecular characterization of a neuronal low-voltage-activated T-type calcium channel. Nature.

Perucca E, Tomson T (2011) The pharmacological treatment of epilepsy in adults. Lancet Neurol.

Pike FG, Goddard RS, Suckling JM, Ganter P, Kasthuri N, Paulsen O (2000) Distinct

frequency preferences of different types of rat hippocampal neurones in response to oscillatory input currents. J Physiol.

Pothmann L, Klos C, Braganza O, Schmidt S, Horno O, Memmesheimer R-M, Beck H (2019) Altered dynamics of canonical feed-back inhibition predicts increased burst transmission in chronic epilepsy. J Neurosci 39:8998–9012.

Pothmann L, Müller C, Averkin RG, Bellistri E, Miklitz C, Uebachs M, Remy S, de la Prida L, Beck H (2014) Function of inhibitory micronetworks is spared by Na+ channel-acting anticonvulsant drugs. J Neurosci 34:9720–9735 Available at: https://www.ncbi.nlm.nih.gov/pubmed/25031410.

Pouille F, Scanziani M (2001a) Enforcement of temporal fidelity in pyramidal cells by somatic feed-forward inhibition. Science (80-) 293:1159–1163 Available at: https://www.ncbi.nlm.nih.gov/pubmed/11498596.

Pouille F, Scanziani M (2001b) Enforcement of temporal fidelity in pyramidal cells by somatic feed-forward inhibition. Science (80-).

Pouille F, Scanziani M (2004a) Routing of spike series by dynamic circuits in the hippocampus. Nature 429:717–723 Available at: http://www.nature.com/doifinder/10.1038/nature02615.

Pouille F, Scanziani M (2004b) Routing of spike series by dynamic circuits in the hippocampus. Nature 429:717–723 Available at: https://www.ncbi.nlm.nih.gov/pubmed/15170216.

Pratt JH, Berry JF, Kaye B, Goetz FC (1969) Lipid class and fatty acid composition of rat brain and sciatic nerve in alloxan diabetes. Diabetes.

Prince HC, Tzingounis A V., Levey AI, Conn PJ (2000) Functional downregulation of GluR2 in piriform cortex of kindled animals. Synapse.

Proddutur A, Yu J, Elgammal FS, Santhakumar V (2013) Seizure-induced alterations in fast-spiking basket cell GABA currents modulate frequency and coherence of gamma oscillation in network simulations. Chaos.

Qu Y, Curtis R, Lawson D, Gilbride K, Ge P, DiStefano PS, Silos-Santiago I, Catterall WA, Scheuer T (2001) Differential modulation of sodium channel gating and persistent sodium currents by the β1, β2, and β3 subunits. Mol Cell Neurosci

18:570–580.

Qu Y, Rogers J, Tanada T, Scheuer T, Catterall WA (1995) Molecular determinants of drug access to the receptor site for antiarrhythmic drugs in the cardiac Na+ channel. Proc Natl Acad Sci 92:11839–11843 Available at: http://www.pnas.org/content/92/25/11839.

Ragsdale DS, Avoli M (1998) Sodium channels as molecular targets for antiepileptic drugs. Brain Res Rev 26:16–28.

Ragsdale DS, McPhee JC, Scheuer T, Catterall WA (1996) Common molecular determinants of local anesthetic, antiarrhythmic, and anticonvulsant block of voltage-gated Na+ channels. Proc Natl Acad Sci 93:9270–9275 Available at: http://www.pnas.org/cgi/doi/10.1073/pnas.93.17.9270.

Rambeck B, Jürgens UH, May TW, Wolfgang Pannek H, Behne F, Ebner A, Gorji A, Straub H, Speckmann EJ, Pohlmann-Eden B, Löscher W (2006) Comparison of brain extracellular fluid, brain tissue, cerebrospinal fluid, and serum concentrations of antiepileptic drugs measured intraoperatively in patients with intractable epilepsy. Epilepsia 47:681–694.

Regesta G, Tanganelli P (1999) Clinical aspects and biological bases of drug-resistant epilepsies. Epilepsy Res 34:109–122.

Remy S, Beck H (2006) Molecular and cellular mechanisms of pharmacoresistance in epilepsy. Brain 129:18–35.

Remy S, Gabriel S, Urban BW, Dietrich D, Lehmann TN, Elger CE, Heinemann U, Beck H (2003a) A novel mechanism underlying drug resistance in chronic epilepsy. Ann Neurol 53:469–479.

Remy S, Urban BW, Elger CE, Beck H (2003b) Anticonvulsant pharmacology of voltage-gated Na+ channels in hippocampal neurons of control and chronically epileptic rats. Eur J Neurosci 17:2648–2658 Available at: https://www.ncbi.nlm.nih.gov/pubmed/12823472.

Rodriguez E, George N, Lachaux JP, Martinerie J, Renault B, Varela FJ (1999) Perception’s shadow: Long-distance synchronization of human brain activity. Nature.

Rogawski MA, Gryder D, Castaneda D, Yonekawa W, Banks MK, Lia H (2003) GluR5 kainate receptors, seizures, and the amygdala. Ann N Y Acad Sci 985:150–162 Available at: http://onlinelibrary.wiley.com/store/10.1111/j.1749-6632.2003.tb07079.x/asset/j.1749-6632.2003.tb07079.x.pdf?v=1&t=i7ernk9l&s=53726bc329f057e0db00b9c83edfb6610b9ff29c.

Rogawski MA, Löscher W (2004) The neurobiology of antiepileptic drugs. Nat Rev Neurosci 5:553–564.

Royeck M, Kelly T, Opitz T, Otte D-M, Rennhack A, Woitecki A, Pitsch J, Becker A, Schoch S, Kaupp UB, Yaari Y, Zimmer A, Beck H (2015) Downregulation of Spermine Augments Dendritic Persistent Sodium Currents and Synaptic Integration after Status Epilepticus. J Neurosci 35:15240–15253 Available at: http://www.jneurosci.org/cgi/doi/10.1523/JNEUROSCI.0493-15.2015.

Rozov A, Burnashev N (1999) Polyamine-dependent facilitation of postsynaptic AMPA receptors counteracts paired-pulse depression. Nature.

Sanchez RM, Koh S, Rio C, Wang C, Lamperti ED, Sharma D, Corfas G, Jensen FE (2018) Decreased Glutamate Receptor 2 Expression and Enhanced Epileptogenesis in Immature Rat Hippocampus after Perinatal Hypoxia-Induced Seizures. J Neurosci.

Sari P, Kerr DS (2001) Domoic acid-induced hippocampal CA1 hyperexcitability independent of region CA3 activity. Epilepsy Res.

Sayin U, Osting S, Hagen J, Rutecki P, Sutula T (2003) Spontaneous seizures and loss of axo-axonic and axo-somatic inhibition induced by repeated brief seizures in kindled rats. J Neurosci.

Scheffer E, Berkovic S, Capovilla G, Connolly MB, French J, Guilhoto L, Hirsch E, Jain S, Mathern GW, Moshé SL, Nordli DR, Perucca E, Tomson T (2017) ILAE classification ofthe epilepsies: Position paper ofthe ILAE Commission for Classification and Terminology. 58:512–521.

Scheffer IE, Berkovic S, Capovilla G, Connolly MB, French J, Guilhoto L, Hirsch E, Jain S, Mathern GW, Moshé SL, Nordli DR, Perucca E, Tomson T, Wiebe S, Zhang

YH, Zuberi SM (2018) ILAE classification of the epilepsies: position paper of the ILAE Commission for Classification and Terminology. Zeitschrift fur Epileptol.

Sheth RD, Gidal BE (1998) Refractory status epilepticus: Response to ketamine. Neurology 51:1765–1766.

Sik A, Penttonen M, Ylinen A, Buzsáki G (1995) Hippocampal CA1 interneurons: an in vivo intracellular labeling study. J Neurosci 15:6651–6665 Available at: https://www.ncbi.nlm.nih.gov/pubmed/7472426.

Sloviter RS (1987) Decreased hippocampal inhibition and a selective loss of interneurons in experimental epilepsy. Science (80-).

Soares-da-Silva P, Pires N, Bonifácio MJ, Loureiro AI, Palma N, Wright LC (2015) Eslicarbazepine acetate for the treatment of focal epilepsy: an update on its proposed mechanisms of action. Pharmacol Res Perspect 3:e00124 Available at: https://www.ncbi.nlm.nih.gov/pubmed/26038700.

Sommer B, Köhler M, Sprengel R, Seeburg PH (1991) RNA editing in brain controls a determinant of ion flow in glutamate-gated channels. Cell.

Sommer C, Roth SU, Kiessling M (2001) Kainate-induced epilepsy alters protein expression of AMPA receptor subunits GluR1, GluR2 and AMPA receptor binding protein in the rat hippocampus. Acta Neuropathol.

Somogyi P, Nunzi MG, Gorio A, Smith AD (1983) A new type of specific interneuron in the monkey hippocampus forming synapses exclusively with the axon initial segments of pyramidal cells. Brain Res.

Stafstrom CE (2007) Persistent Sodium Current and Its Role in Epilepsy. Epilepsy Curr.

Subramaniam S, Rho JM, Penix L, Donevan SD, Fielding RP, Rogawski M a (1995) Felbamate block of the N-methyl-D-aspartate receptor. J Pharmacol Exp Ther 273:878–886.

Szabo A, Somogyi J, Cauli B, Lambolez B, Somogyi P, Lamsa KP (2012) Calcium-Permeable AMPA Receptors Provide a Common Mechanism for LTP in Glutamatergic Synapses of Distinct Hippocampal Interneuron Types. J Neurosci 32:6511–6516 Available at:

http://www.jneurosci.org/cgi/doi/10.1523/JNEUROSCI.0206-12.2012.

Szobota S, Gorostiza P, Del Bene F, Wyart C, Fortin DL, Kolstad KD, Tulyathan O, Volgraf M, Numano R, Aaron HL, Scott EK, Kramer RH, Flannery J, Baier H, Trauner D, Isacoff EY (2007) Remote Control of Neuronal Activity with a Light-Gated Glutamate Receptor. Neuron.

Talley EM, Cribbs LL, Lee JH, Daud A, Perez-Reyes E, Bayliss DA (1999) Differential distribution of three members of a gene family encoding low voltage-activated (T-type) calcium channels. J Neurosci.

Taylor DC (1989) The Neuropathology of Temporal Lobe Epilepsy. By C. J. Bruton. (Pp. 158; illustrated; £20.00.) Oxford University Press: Oxford. 1988. Psychol Med.

Thomas Klausberger, Peter Somogyi (2008) Neuronal Diversity and Temporal Dynamics: The Unity of Hippocampal Circuit Operations. Science (80-).

Tremblay E, Represa A, Ben-Ari Y (1985) Autoradiographic localization of kainic acid binding sites in the human hippocampus. Brain Res.

Trimmer JS, Rhodes KJ (2004) Localization of voltage-gated ion channels in mammalian brain. Annu Rev Physiol 66:477–519 Available at: https://www.ncbi.nlm.nih.gov/pubmed/14977411.

Turski L, Ikonomidou C, Turski WA, Bortolotto ZA, Cavalheiro EA (1989) Review: Cholinergic mechanisms and epileptogenesis. The seizures induced by pilocarpine: A novel experimental model of intractable epilepsy. Synapse.

Turski WA, Cavalheiro EA, Bortolotto ZA, Mello LM, Schwarz M, Turski L (1984) Seizures produced by pilocarpine in mice: A behavioral, electroencephalographic and morphological analysis. Brain Res.

Turski WA, Cavalheiro EA, Schwarz M, Czuczwar SJ, Kleinrok Z, Turski L (1983) Limbic seizures produced by pilocarpine in rats: Behavioural, electroencephalographic and neuropathological study. Behav Brain Res.

Uebachs M, Opitz T, Royeck M, Dickhof G, Horstmann M-T, Isom LL, Beck H (2010) Efficacy Loss of the Anticonvulsant Carbamazepine in Mice Lacking Sodium Channel Subunits via Paradoxical Effects on Persistent Sodium Currents. J

Neurosci.

Ulbricht W (2005) Sodium channel inactivation: Molecular determinants and modulation. Physiol Rev.

Vacher H, Mohapatra DP, Trimmer JS (2008) Localization and targeting of voltage-dependent ion channels in mammalian central neurons. Physiol Rev 88:1407–1447 Available at: https://www.ncbi.nlm.nih.gov/pubmed/18923186.

Van Vliet EA, Aronica E, Tolner EA, Lopes Da Silva FH, Gorter JA (2004) Progression of temporal lobe epilepsy in the rat is associated with immunocytochemical changes in inhibitory interneurons in specific regions of the hippocampal formation. Exp Neurol.

Van Vreeswijk C, Abbott LF, Bard Ermentrout G (1994) When inhibition not excitation synchronizes neural firing. J Comput Neurosci.

Verdoorn TA, Burnashev N, Monyer H, Seeburg PH, Sakmann B (1991) Structural determinants of ion flow through recombinant glutamate receptor channels. Science (80-).

Vida I, Halasy K, Szinyei C, Somogyi P, Buhl EH (1998) Unitary IPSPs evoked by interneurons at the stratum radiatum-stratum lacunosum-moleculare border in the CA1 area of the rat hippocampus in vitro. J Physiol.

Wang XJ, Buzsáki G (1996) Gamma oscillation by synaptic inhibition in a hippocampal interneuronal network model. J Neurosci.

Whitaker WRJ, Faull RLM, Dragunow M, Mee EW, Emson PC, Clare JJ (2001) Changes in the mRNAs encoding voltage-gated sodium channel types II and III in human epileptic hippocampus. Neuroscience 106:275–285.

Whittington MA, Traub RD (2003) Interneuron diversity series: inhibitory interneurons and network oscillations in vitro. Trends Neurosci 26:676–682 Available at: https://www.ncbi.nlm.nih.gov/pubmed/14624852.

Whittington MA, Traub RD, Jefferys JGR (1995) Synchronized oscillations in interneuron networks driven by metabotropic glutamate receptor activation. Nature.

WHO (2018) Epilepsy - Key facts. WHO:1 Available at: http://www.who.int/en/news-room/fact-sheets/detail/epilepsy.

Wiestler O, Blumcke I (2002) Introduction: Pathogenesis and Pathophysiology of Focal Epilepsies. Brain Pathol:191–192 Available at: http://www3.interscience.wiley.com/journal/118923902/abstract%5Cnpapers2://publication/uuid/DC0D1A7F-A57E-420C-99E7-5DE56AF17ACC.

Wisden W, Seeburg PH (1993) Mammalian ionotropic glutamate receptors. Curr Opin Neurobiol.

Wittner L, Maglóczky Z, Borhegyi Z, Halász P, Tóth S, Eross L, Szabó Z, Freund TF (2001) Preservation of perisomatic inhibitory input of granule cells in the epileptic human dentate gyrus. Neuroscience.

Worrell GA, Gardner AB, Stead SM, Hu S, Goerss S, Cascino GJ, Meyer FB, Marsh R, Litt B (2008) High-frequency oscillations in human temporal lobe: Simultaneous microwire and clinical macroelectrode recordings. Brain.

Worrell GA, Parish L, Cranstoun SD, Jonas R, Baltuch G, Litt B (2004) High-frequency oscillations and seizure generation in neocortical epilepsy. Brain.

Wozny C, Gabriel S, Jandova K, Schulze K, Heinemann U, Behr J (2005) Entorhinal cortex entrains epileptiform activity in CA1 in pilocarpine-treated rats. Neurobiol Dis.

Yamamoto J, Suh J, Takeuchi D, Tonegawa S (2014) Successful execution of working memory linked to synchronized high-frequency gamma oscillations. Cell.

Yu FH, Mantegazza M, Westenbroek RE, Robbins CA, Kalume F, Burton KA, Spain WJ, McKnight GS, Scheuer T, Catterall WA (2006) Reduced sodium current in GABAergic interneurons in a mouse model of severe myoclonic epilepsy in infancy. Nat Neurosci 9:1142–1149.

Yu J, Proddutur A, Elgammal FS, Ito T, Santhakumar V (2013) Status epilepticus enhances tonic GABA currents and depolarizes GABA reversal potential in dentate fast-spiking basket cells. J Neurophysiol.

Eidesstattliche Erklärung

Hiermit versichere ich, dass diese Dissertation – abgesehen von den ausdrücklich bezeichneten Hilfsmitteln – persönlich, selbständig und ohne Benutzung anderer als der angegebenen Hilfsmittel angefertigt wurde. Die aus anderen Quellen direkt oder indirekt übernommenen Daten und Konzepte sind unter Angabe der Quelle kenntlich gemacht. Die vorgelegte Arbeit ist nicht bereits anderweitig als Dissertation eingereicht worden. Für die Erstellung der vorgelegten Arbeit und/oder die Gelegenheit zur Promotion wurde keine fremde Hilfe, insbesondere keine entgeltliche Hilfe von Vermittlungs- bzw. Beratungsdiensten (Promotionsberatern / -vermittlern oder anderen Personen) in Anspruch genommen.

Bonn, den

Sarah Schmidt

Acknowledgments

Zu aller erst möchte ich Herrn Prof. Dr. Heinz Beck meinen großen Dank aussprechen. Ich bin ihm sehr dankbar für die Möglichkeit meine Doktorarbeit in seinem Labor erarbeiten zu können. Ich schätze seinen respektvollen und wertschätzenden Umgang mit mir und allen Mitarbeitern. Ich konnte ihn immer um Rat fragen und er unterstützte mich in all meinen Entscheidungen. Für seine fürsorgliche Betreuung bin ich außerordentlich dankbar.

Als mein Zweitbetreuer setzte sich Prof. Dr. Walter Witke sehr für mich ein und ermöglichte mir zusammen mit Herrn Prof. Dr. Heinz Beck meine Doktorarbeit an der Mathematisch-Naturwissenschaftliche Fakultät zu schreiben. Für seinen Einsatz und seine Betreuung möchte ich mich bedanken.

Außerdem möchte ich Prof. Dr. Jörg Höhfeld und Prof. Dr. Christa Müller für ihre Teilnahme und ihren Einsatz in meiner Promotionskommission danken.

Ein besonderer Dank geht an Dr. Thoralf Opitz. Er hat mich stets unterstützt und war nicht müde, mir jede meiner abertausenden Fragen zu beantworten. Außerdem möchte ich mich auch bei Dr. Tony Kelly und Dr. Laura Ewell für ihr wertvolles Feedback bedanken. Die gemeinsamen Diskussionen über meine Arbeit waren sehr hilfreich für meine wissenschaftliche Entwicklung.

Mir war es außerdem eine Freude zusammen mit Dr. Dominik Holtkamp zu arbeiten. Wir durften einige Stunden gemeinsam bei Experimenten verbringen und ohne ihn wären sie nur halb so unterhaltsam gewesen.

Diese Arbeit wäre auch nicht möglich gewesen durch die immerzu dagewesene Hilfe von Margit Reitze, Sabrina Walch, Nicole Schönfelder, Rebecca Zölzer und Lea Keller. Ganz egal ob im technischen oder organisatorischen Bereich, ihr wart mir immer eine große Unterstützung.

Neben der Laborarbeit gehört auch die Arbeit im Büro zu der Erstellung einer Doktorarbeit. Ich kann mir keinen besseren Sitznachbarn vorstellen als Kristian Reichelt. Ich schätze jedes unserer Gespräche, ob über wissenschaftliche Themen, Politik, Urlaub oder ganz banale Empfindlichkeiten.

Ein ganz besonderer Dank geht an mein Azizam Negar Nikbakht. Ich kann mir nicht vorstellen, wie die Jahre der Doktorarbeit ohne dich gewesen wären. Ich vermisse jetzt schon unser morgendliches Café-Date. Unsere gemeinsame Reise in den Iran hat uns eng zusammengeschweißt und ich werde dir ewig dankbar dafür sein, dass du Einblicke deines Heimatlandes mit mir geteilt hast. Ich hoffe wir werden noch unendlich viele Reisen gemeinsam erleben.

Ich möchte auch der gesamten AG Beck danken. Wir haben gemeinsam wunderbare Momente erlebt, ob beim Bier-Tasting, bei einer aufregenden Kanu-Fahrt, auf Studentensymposien, bei Konferenzbesuchen oder Weihnachtsmarkttreffen. Ich habe die familiäre Atmosphäre sehr genossen und werde euch alle vermissen.

Diese Doktorarbeit wäre auch nicht möglich gewesen ohne die Unterstützung abseits vom Arbeitsplatz. Besonderer Dank geht an meine Freunde, mit denen ich immer reden konnte, wenn etwas auch mal nicht so gut lief. Unsere Ausflüge, ob in die Alpen, an die Mosel, Wochenenden in Portugal oder Weihnachtsmarktbesuche in Nürnberg waren eine wunderbare Zeit und ich freue mich auf mehr in der Zukunft. Kurz vor dem Beginn meiner Doktorarbeit durfte ich auch einen ganz besonderen Menschen kennen lernen. Simon, jetzt kennen wir uns schon über 5 Jahre und wir haben gemeinsam zwei Doktorarbeiten erlebt. Du hast mich immer unterstützt. Durch dich bin ich zu einer besseren Version meiner selbst geworden. All die wunderbaren Erfahrungen, ob gemeinsam den Triglav erklimmen, einen Halbmarathon laufen oder nach Berlin ziehen, mit dir habe ich vor nichts Angst.

Meiner Familie steht mein größter Dank zu. Mama und mein liebster Bruder Jani, ihr wart immer meine Stütze und ich wäre ohne euch nie so weit gekommen. Ihr habt immer an mich geglaubt und mich gestärkt, wenn ich unsicher war. Mama und Papa, ihr habt mich zu dem Menschen gemacht, der ich heute bin. Ich bin so dankbar für die Liebe, die ihr mir immer habt zukommen lassen. Durch eure Unterstützung weiß ich, dass ich alles erreichen kann was ich mir vornehme. Papa, ich weiß du warst immer unglaublich stolz auf mich und ich wünschte mir sehr, diesen Moment mit dir teilen zu können. Aber ich weiß, dass ein Teil von dir immer bei mir sein wird und ich werde ihn in Ehren halten.